LUMINOL LUMINESCENCE-BASED THERANOSTICS FOR PRE-CLINICAL BREAST ADENOCARCINOMA

by

HAMAD S. ALSHETAIWI

B.A., Qassim University, Saudi Arabia, 2006

A THESIS

submitted in partial fulfillment of the requirements for the degree

MASTER OF SCIENCE

Department of Anatomy & Physiology
College of Veterinary Medicine

KANSAS STATE UNIVERSITY
Manhattan, Kansas

2014

Approved by:
Major Professor
Deryl L Troyer

Copyright

Abstract

Breast cancer ranks second as a cause of cancer death in women in the USA. Detection of early tumors and tumor-targeted treatments could decrease the problems associated with breast cancer management. Photodynamic therapy (PDT) is a cancer treatment that uses a photosensitizer and a specific wavelength of light and is currently in clinical trials for breast cancer. When tumor cells which have absorbed photosensitizer are exposed to the correct wavelength of light, reactive oxygen species are generated, resulting in tumor cell death. Poor tissue penetration of light is a major limitation in PDT, restricting its use to treatment of localized tumors. Light generation at the tumor area might increase the effectiveness of PDT. Polymorphonuclear neutrophils (PMNs) are known to often infiltrate breast adenocarcinoma, and their activatation in tumor stroma produces luminescence in the presence of luminol. Here, we hypothesized that luminol can be used as a theranostic agent for luminescence-based early tumor detection (diagnosis) and *in situ* PDT (treatment). BALB/c mice were transplanted with 4T1 mammary adenocarcinoma cells to establish a breast adenocarcinoma model. The early tumor detection objective was tested by daily intraperitoneal injection of luminol and *in vivo* luminescence imaging. To test the PDT treatment objective,the photosensitizer 5-aminolevulinic acid (ALA) and luminol were administered to mice through intraperitoneal and intravenous routes, respectively. This treatment regimen was repeated six times and ALA alone/luminol alone/saline treated tumor-bearing mice were used as controls. Results demonstrated that luminol allowed detection of activated PMNs only two days after 4T1 cell transplantation, even though tumors were not yet palpable. Relative differences in the increase of tumor volume and final tumor weights were analyzed to test the *in situ* PDT. Analysis of the data showed luminol

treatments resulted in breast adenocarcinoma tumor growth attenuation. In conclusion this study provides evidence that luminol can be a theranostic agent for breast adenocarcinoma.

Table of Contents

List of Figures

Acknowledgements

First of all, my special thanks go to my parents, Saleh and Norh, who taught me at every step through my life and shaped me into the person that I am today. Also, I would like to thank my whole family for providing me all the support needed in order to succeed in my studies.

I would like to express my deepest gratitude to my major professor, Dr. Deryl Troyer, for the many opportunities given to me as a graduate student to obtain experiences in the scientific field. His suggestions, guidance and support maintained my attention and raised my abilities. I would like to extend my thanks and appreciation to my committee members, Dr. Stefan Bossmann and Dr. Duane Davis, for the teaching, encouragement, assistance and their time to guide me during my master's program.

Special thanks go to Marla Pyle for all her help and support in my research projects and made me comfortable in the lab during my researches. I would like to thank our lab members, Dr. Tej Shrestha, Dr. Matthew T. Basel, Dr. Sivasai Balivada and Dr. Mausam Kalita for their help and valuable input in my research projects. Without them many of my projects would have stumbled. I would also like to thank members of the KSU chemistry department for their help in some of my research projects: Dr. Bossmann's lab members Sebastian Wendel, Dr. Hongwang Wang, and Dr. Thilani Samarakoon and Dr. Daniel Higgins and his lab member Dipak Giri. Also, I would like to acknowledge College of Medicine, University of Ha'il, Saudi Arabia for the financial support throughout my studies.

Finally, I greatly thank my nephew and roommate Muhannad Alshetaiwi, and my graduate friends Sivasai Balivada, Sebastian Wendel, Sailesh Menon, Yelican Rodrigues,

Jodi Morton, Oian Wang, and Lakshmi Deepthi Uppalapati for all their support and encouragement in my most difficult moments during my graduate school.

Chapter 1 - Introduction

Cancer is a worldwide disease and causes 1 of 8 deaths in all countries. For instance, the International Agency for Research on Cancer estimated around 12.7 million new cancer cases and 7.6 million people will die of cancer worldwide in 2008. Also, it is expected that these numbers will double to 21.4 million new cases and 13.15 million deaths in 2030 [1]. Many research teams around the world are working very hard to develop new approaches in cancer detection and therapy. Even with these advancements in cancer research we still need to understand more about cancer; thus, this mission has not completed yet [2, 3]. Cancer begins in the cells of body by uncontrolled growth of abnormal cells. Normal body cells grow and divide to form new cells and replace old cells that die. However, when normal cells become mutated, they lose the ability to control division or undergo apoptosis [4]. Thus, these mutated cells become cancer cells and begin to grow and divide until they form a tumor, which may invade surrounding tissues, or travel to distant sites by a mechanism called metastasis [3].

Breast cancer

Breast cancer is the most common cancer in women worldwide. In the USA, breast cancer ranks as the second cause of cancer death in women [5]. The American Cancer Society estimates that 232,340 of women will be diagnosed with breast cancer and about 39,620 women will die because of breast cancer in the US in 2013 [5]. Breast cancer is described as a malignant tumor which begins in the epithelial cells that line the ducts and lobules of the breast [2, 6]. Most breast cancers are carcinomas and divided into two major types, *in situ* carcinomas and invasive (or infiltrating) carcinomas [7]. Breast adenocarcinoma describes one type of carcinoma that begins in the glandular ducts or lobules of the breast tissue [2]. The breast has a

lot of sections called lobes and these lobes are connected to thin tubes called ducts. The most common type of breast cancer is ductal cancer and the other type of breast cancer is called lobular cancer. Additionally, there is a rare type of breast cancer called inflammatory breast cancer which is characterized by general inflammation of the breast [2].

In the beginning of breast cancer, abnormal cells form *in situ* carcinomas in either lobes or ducts with no invasion [6, 7]. In some cases these cancer cells extend and become invasive (or infiltrative) ductal or lobular carcinomas. Thus, cancer cells spread to the skin and/or chest wall of the breast and may spread to lymph nodes [6, 7].

Subsequently, these breast cancer cells become aggressive and have the ability to metastasize to other parts of the body through the lymphatic system and blood stream [6]. Therefore, cancer cells will be metastasized to other organs of the body such as bones, lung, liver, or brain [6].

The Tumor microenvironment

A tumor is a complex tissue comprising not only cancer cells. It is a disorganized organ containing numerous different types of cells [8]. Cancer cells are the foundation of the disease and can instruct surrounding cells to contribute to malignant tumor formation [8]. Cancer cells and stromal cells during tumor growth are known to secrete numerous cytokines to attract different type of cells like immune cells, angiogenic vascular cells, and fibroblast cells into the tumor environment [3, 9]. Some examples of cytokines secreted during tumorigenesis are interleukins (IL-6 and IL-8), interferons (IFN-γ, INF-α, INF-β), and tumor necrosis factor-α (TNF-α) [10]. It has been reported that neutrophil granulocytes migrate to a variety of tumors such as breast cancer, prostate cancer and glioma during tumorigenesis in animals and humans

[11]. These reports suggest that tumor tissues have different features from normal tissue. Thus, these features could potentially be used for tumor detection and treatment.

Cancer therapy

Earlier in the 20th century, surgery was the only treatment available for cancer patients. The first description of cancer surgery was attributed to Ephraim Mcdowell in 1809 when he removed an ovarian tumor [11]. Then, in 1894 William Hasted introduced radical mastectomy for breast cancer [11]. Furthermore, Hasted suggested removing surrounding tissues to remove all cancer cells. After that, in 1968 Bernard Fisher described that breast cancer cells can migrate to the bloodstream and lymphatic tissues [11]. Additionally, Fisher demonstrated that using surgery to remove the primary tumor mass is not enough for cancer treatment. He suggested using a combination of radical mastectomy and radiation therapy or chemotherapy. In 1928 was the first use of radiation therapy in head and neck cancers to render it curable [11]. Around 1948, Sidney Farber reported folic acid anticancer drugs as a chemotherapy which could be used to treat childhood leukemia [11]. Although many developments in cancer therapy have taken place during the nineteenth and twentieth centuries, most of these therapies cause side effects.

Cancer cells are known to grow and divide faster than many normal cells. Consequently, present cancer therapies like chemotherapy and radiation target dividing cells [12] [13]. However, some normal progenitor cells divide quickly, for example, cells lining the digestive tract and hematopoietic stem cells [14]. In this case chemotherapy and radiation therapy affect these normal cells; high doses will cause GI disturbances and immunosuppression [15].

The main goal of cancer therapy should be not only to kill primary tumor cells but at the same time to activate the immune system to identify and terminate any remaining tumor cells [15]. Consequently, different research teams are trying to develop varieties of targeting

treatments which might have these desirable properties; among these are photodynamic therapy, hyperthermia, and cryotherapy [15]. Different studies reported that those tumor-targeted treatments can cause inflammatory response and recruit immune cells such as dendritic cells, neutrophils, macrophages and lymphocytes [15]. Cancer therapy today has changed from a decade ago. Now the tumor microenvironment, interactions between cells, secreted factors and cytokines are the main response to cancer treatment [16].

Photodynamic therapy

Early Egyptian, Indian and Chinese civilizations have used light as a therapeutic agent to treat a variety of diseases such as skin cancer, rickets, psoriasis and vitiligo [17]. Herodotus was a Greek physician who suggested that exposure of the body to the sun might restore health [18]. In the 19th century the term "phototherapy" was developed when Niel Finsen used red light to treat smallpox. Therefore, in 1903, Finsen was awarded a Nobel Prize for his discovery [17]. In the same year, Von Tappeiner and Jasionek used the chemical eosin with white light to treat skin cancer [17]. Then in 1907, Von Tappeiner demonstrated that oxygen is involved with a photosensitizer reaction and called this phenomenon "photodynamic action" [17].

In 1913, Friedrich Meyer-Betz, a German scientist, used a photosensitizer, hematoporphyrin, on his hands and noticed swelling and pain after light exposure [17]. Later, in 1972, Diamond suggested that the use of tumor-localizing and phototoxic properties of prophyrins might kill cancer cells. In 1975, Dougherty reported that hematoporphyrin in the presence of red light treated breast cancer in mice [19]. In the same year, Kelly demonstrated a similar result in bladder cancer. One year later he started the first human trial with hematoporphyrin [20, 21]. During 1980s, photodynamic therapy was examined for a variety of human tumors, such as lung, stomach, head, neck, breast, and brain [18]. In 1993, the first

approved trial of PDT in Canada to treat bladder cancer by using the photosensitizer Photofrin took place. In 2003, the photosensitizers 5-aminolevulinic acid and Foscan passed through clinical trials and were approved for use in the European Union [17].

Briefly, the mechanism of photodynamic therapy starts when a non-toxic photosensitizer is introduced to the body and accumulate in the cancer cells [17]. This is followed by exposure to a specific wavelength of light that can be absorbed by photosensitizer within cancer cells. Then, activation of the photosensitizer causes it to transfer its energy to tissue oxygen to generate reactive oxygen species (ROS) [17]. These ROS mediate cellular toxicity by attacking cell organelles; disrupting regular cell function and leading to cell death. (**Chapter 3** contains more details of PDT mechanisms.)

Cancer therapies such as surgery, chemotherapy and radiation therapy often have a high rate of complications [22]. Therefore, PDT has numerous advantages and could be another choice of treatment. PDT has low toxicity, high specificity, and it can be repeated several times without causing toxicity or resistance [22]. Also, it can be combined with other therapies. These advantages make PDT a good treatment for small localized superficial tumors on the skin [22]. In contrast, PDT has some limitations. For example, most wavelengths of light that have been used in PDT cannot penetrate the skin more than a few millimeters. For that reason, PDT cannot be used to treat deep or metastasized tumors [23].

Cancer detection

Detecting tumors at earlier stages could significantly improve therapeutic outcomes. For instance, the 5-year relative survival of breast cancer decreases to 23.4 percent when the cancer was discovered at the distant stage, from 83.6 percent at the regional stage and 98 percent at the localized stage [24]. Understanding the tumor microenvironment may facilitate tumor diagnosis

at the earliest stages [10]. Different research teams demonstrated that the tumor microenvironment is different from normal tissue because it is often characterized by low pH, hypoxia, over-expressed proteases, and infiltration of defensive and immune cells [10].

Several imaging techniques have been used to examine the tumor microenvironment. Cancer imaging technologies have become essential tools in cancer research, medical use, and clinical trials [25]. Different imaging tools that have been developed since 1950 include computed tomography (CT), positron emission tomography (PET), magnetic resonance imaging (MRI), and optical imaging [16]. Imaging technologies like CT, PET and MRI are highly sensitive and quantitative. However, the disadvantages of those instruments are that patients might be exposed to radiation, they are expensive, and they require specialized personnel to monitor and interpret them [25]. On the other hand, optical imaging such as fluorescence imaging and bioluminescence imaging are non-invasive, simple, less expensive, and have short acquisition times. The disadvantages of optical imaging are that they are not quantitative and tissue penetration is poor [25].

Fluorescence imaging was known in the middle of 20^{th} century. In 1942, after intravenous injection of porphyrins red fluorescence was observed in tumors. The first use of green fluorescent fluorescein to detect brain tumors was in 1948. Fluorescence imaging works when a fluorochrome absorbs light at specific wavelength and emits fluorescent light, which can be detected by a CCD camera. Green fluorescent protein (GFP) from jellyfish is the most common protein been used for this technique [25].

Bioluminescence imaging (BLI)

BLI is a non-invasive imaging technique used in pre–clinical studies to image tumors by generating visible light, usually by employing luciferase-expressing cells. Firefly luciferase

(FLuc) is from firefly, *Photinus pyralis* [25]. Administration of the substrate D-luciferin in the presence of adenosine tri-phosphate (ATP), magnesium (Mg^{2+}) and molecular oxygen (O_2) creates oxy-luciferin which can emit light photons at a wavelength about 560nm [10, 25]. Other examples of luciferases include *Renilla reniformis* luciferase (RLuc) and *Gaussia princeps* luciferase (Gluc) which can emit light after addition of the substrate coelenterazine. FLuc, RLuc and Gluc are not toxic, and the light coming out from these systems could be used for diagnostic and therapeutic purposes [25, 26]. The advantage of BLI is that there is no background noise like in fluorescence imaging, thus making this technique highly sensitive [25, 26].

Luminol is described as a chemiluminescent molecule (5-amino-2,3-dihydrophthalazine-1,4-dione) that emits light at maximum of 425 nm when oxidized [10]. Luminol has been used to examine the role of granulocyte-derived reactive oxygen species in heart muscle damage and leukocyte activity in patients with peritonitis [10]. Also, it can detect phagocytic oxidative bursts and subsequent myeloperoxidase (MPO) activity. Additionally, inflamed tissues such as cancer are populated by cells such as neutrophils, monocytes, and macrophages which can produce reactive oxygen species (ROS) by respiratory bursts. These ROS can react with luminol and produce light.

Theranostics

Theranostics is a new approach introduced by Funkhouser in 2002 which combines cancer detection and therapy. The definition of theranostic is a delivery of therapeutic drugs and diagnostic imaging agents to the tumor site at the same time with the same dose [27]. Theranostics as a field is still young but is developing rapidly. Different research groups have developed nanoparticle-based systems such as magnetic nanoparticles for MRI, hyperthermia and delivery of chemotherapeutics for cancer imaging and therapy [27]. PDT is another

approach which has been useful for theranostics. However, even with improvements and the advance studies that have been done in the theranostics field, it has not yet been extended to clinical trials [27]. Based on this background, we hypothesized in this dissertation that luminol can be used as a theranostic agent for luminescence-based early tumor detection (diagnosis) and *in situ* photodynamic therapy (treatment).

Chapter 2 - Luminol-based Bioluminescence Imaging of Mouse Mammary Tumors

Based on the following publication:

Alshetaiwi H, Balivada S, Shrestha T, Pyle M, Basel M, Bossmann S, Troyer D: Luminol-based bioluminescence imaging of mouse mammary tumors. Journal of Photochemistry and Photobiology B: Biology 127:223-228, 2013.

Abstract

Polymorphonuclear neutrophils (PMNs) are the most abundant circulating blood leukocytes. They are part of the innate immune system and provide a first line of defense by migrating toward areas of inflammation in response to chemical signals released from the site. Some solid tumors, such as breast cancer, also cause recruitment and activation of PMNs and release of myeloperoxidase. In this study, we demonstrate that administration of luminol to mice that have been transplanted with 4T1luc2 mammary tumor cells permits the detection of myeloperoxidase activity, and consequently, the location of the tumor. Luminol allowed detection of activated PMNs only two days after cancer cell transplantation, even though tumors were not yet palpable. In conclusion, luminol-bioluminescence imaging (BLI) can provide detection of solid tumors at an early stage in preclinical tumor models.

Introduction

Cancer is a major cause of disease and death in the United States and other countries around the world. For example, the American Cancer Society estimates that 580,350 people will die of cancer in the U.S. in 2013 [28]. Detecting tumors at earlier stages could significantly improve therapeutic outcomes [29, 30]. In pursuing this goal, understanding the tumor microenvironment may facilitate tumor diagnosis at the earliest stages. It has been known that the tumor microenvironment differs from that of normal tissue in that it is often characterized by low pH, hypoxia, over-expressed proteases [31], and is infiltrated by defensive and immune cells [32].

These features can potentially be exploited for detection and treatment. Several imaging techniques have been used to examine the tumor microenvironment, including optical imaging, positron emission tomography (PET) and magnetic resonance imaging (MRI) [25, 31, 33-38] Bioluminescence imaging (BLI) is a non-invasive imaging technique used in pre–clinical oncology research to image tumors by generating visible light, that is usually generated by luciferase-expressing cells [29, 39]. The luciferase-based BLI mechanism involves the oxidation of luciferin in the presence of adenosine tri-phosphate (ATP), magnesium (Mg^{2+}) and molecular oxygen (O_2) to create an electronically excited oxy-luciferin, which emits visible radiation in the yellow-green to yellow-orange spectrum, with an emission maximum of 560nm [29, 39]. Firefly luciferase transfected mouse mammary gland tumor cells 4T1-luc2 show stable light emission in the presence of luciferin and permit the detection of early tumors [29]. In contrast to luciferase-based BLI mechanism, Liu et al., showed beta galactosidase based chemiluminescent imaging for in vivo detection of tumors expressing a beta galactosidase transgene[40] . However, naturally occurring cancers do not express luciferase. Therefore, luciferase-based BLI is not

available when treating cancers in humans and/or non-transfected tumors in mammals. Note that in the research reported here, luciferase-based BLI is only used to define the region of interest.

Luminol (5-amino-2,3-dihydrophthalazine-1,4-dione) is a known chemiluminescent molecule that emits light at a maximum of 425 nm when oxidized [41, 42]. Luminol has been used in various fields, such as biochemistry, analytical chemistry, and clinical diagnostics for detecting reactive intermediates [43]. For instance, luminol has been used as an analytical tool to examine the role of granulocyte-derived reactive oxygen species in heart muscle damage, to screen polymorphonuclear leukocyte function in patients with diabetes mellitus, and to detect leukocyte activity in patients with peritonitis [41, 44]. Luminol detects phagocytic oxidative bursts and subsequent myeloperoxidase (MPO) activity [43]. Gross et al. have demonstrated that luminol-based imaging can be used for quantitative longitudinal monitoring of MPO activity in animal models of acute dermatitis, mixed allergic contact hypersensitivity, focal arthritis and spontaneous large granular lymphocytic tumors [43]. The work presented here consists of tailoring their detection method for revealing early breast tumors (4T1) in mice. Chronically inflamed tissues like cancer are populated by defensive cells, such as neutrophils, monocytes, and macrophages, which can produce reactive oxygen species (ROS) by respiratory bursts and subsequent chemical reactions. Many of these ROS react with luminol and produce light by means of luminol chemiluminescence [45]. Since this chemiluminescence occurs from a chemical and oxidizers that are produced by enzymes in living cells, we will use the term luminol-based bioluminescence imaging (BLI). Here, we present first evidence that administration of luminol to mice that have been transplanted with 4T1 mammary tumor cells permits early stage imaging of tumors by bioluminescence-based detection of MPO activity.

Theory of Luminol-Based Bioluminescence

When PMNs are activated in inflamed tissues such as tumors, they start releasing myeloperoxidase (MPO) [46, 47]. MPO is an abundant protein produced in azurophilic granules of neutrophils, where it can constitute more than 5% of the granule's protein [48]. Respiratory burst is initiated by phagocytic NADPH oxidase (Phox). Phox reduces molecular oxygen (O_2) to give superoxide anions ($O_2^{\cdot -}$). In the presence of protons (H^+), the superoxide anion reacts to the hydroperoxy free radical ($HO_2^{\cdot}$). Superoxide and hydroperoxy free radicals disproportionate to hydrogen peroxide (H_2O_2) and molecular oxygen [49]. Superoxide dismutase (SD) accelerates this reaction. During PMN activation, MPO catalyzes the reaction of H_2O_2 and chloride ions (Cl^-) to produce hypochlorous acid (HOCI) [43]. In turn, HOCI can oxidize luminol, which triggers chemiluminescence [43]. MPO can also directly utilize superoxide anion as a substrate for peroxidase-catalyzed oxidation of luminol [43]. The manifold of reactions is shown in (Figure 2-1).

Luminol can detect activated neutrophils, which often accumulate in tumor tissue. Therefore, luminol may be a clinically relevant method for detecting tumors in vivo. To verify the ability of luminol to detect tumors, 4T1 tumors bearing a firefly luciferase gene were generated in Balb/c mice. Luciferin/luciferase is a well-known imaging system that can detect luciferase bearing cells very specifically in vivo. Luciferase detection is clinically irrelevant, though, because clinical tumors do not contain luciferase genes. If luminol imaging could produce images comparable to luciferin in luciferase bearing tumors it would be validated as a tumor detection system. Therefore, luminol bioluminescence was compared to the highly-sensitive but clinically-irrelevant luciferin bioluminescence. We were able to demonstrate using

4T1luc2 tumors in BALB/c mice that MPO detection from neutrophils is especially suited to image tumors very early after implantation.

Material and Methods

Materials and Cell Culture

Mouse mammary gland adenocarcinoma tumor cell line 4T1luc2 was purchased from Caliper Life Sciences, Hopkinton, MA. This cell line has been engineered to stably express the firefly luciferase gene luc2 [50]. Cells were grown in RPMI1640 medium supplemented with 10% fetal bovine serum (FBS; Sigma-Aldrich, St. Louis, MO) and 1% penicillin/ streptomycin (Invitrogen, Grand Island, NY). Cells were incubated at 37°C at 95% humidity in a 5% CO_2 incubator. Luminol sodium salt was purchased from Gold Biotechnology Inc., St. Louis, MO. Luciferin was purchased from Caliper Life Sciences. Diff-Quick staining kit was obtained from IMEB Inc., San Marcos, CA. Red blood cells (RBC) lysis buffer, bovine serum albumin (BSA) and phorbol myristate acetate (PMA) were acquired from Sigma-Aldrich, St. Louis, MO. PE conjugated rat anti-mouse Ly-6G or isotype were bought from BD Biosciences, San Jose, CA.

ex vivo experiments

Differential count

To confirm the increase in neutrophil percentage in circulating white blood cells (WBCs), $1X10^5$ 4T1luc2 tumor cells in 25µL phosphate buffered saline (PBS) were transplanted into mammary fat pad number 7 of 3 BALB/C mice. Three to four drops of blood was collected from the tail vein of these mice on day 1 and 8 after tumor cell transplantation followed by blood smear preparation. Smears were air dried and stained with Diff Quick staining kit to identify

nucleated cells. Differential blood count was conducted for 100 WBCs on each smear and the estimated relative circulating neutrophil percentage was compared between day 1 and 8.

Flow cytometry

Ly6G is a membrane bound protein expressed on granulocytes and has been used to determine neutrophil percentage in circulating WBCs. To validate differential count results, direct immunofluorescence staining was conducted on mouse blood by using PE-Ly6G antibody. For blood collection, four BALB/C mice were divided into two groups on day 0. The control group was injected with 25 µl PBS and the treatment group was injected with $1X10^5$ 4T1luc2 cells in 25 µl PBS into mammary fat pad number seven. On days 3, 6, and 12 after tumor cell transplantation, approximately 100ul of blood was collected from each mouse by submandibular (cheek-pouch) bleeding. To prevent non-specific binding of immunoglobulins, blood samples were incubated for 10 min with 20% mouse serum in 1% BSA. After blocking, samples were stained with PE-Ly-6G antibody or isotype control for 30 min in the dark at 4°C. Samples were treated with RBC lysis buffer and analyzed by using a Sony EC800 flow cytometer (Sony Biotechnology Inc., Champaign, Illinois). A 488 nm laser was used for excitation and a 585 nm optical filter (FL2) was used to collect emitted PE fluorescence. Healthy leukocytes were gated by plotting forward scatter (FSCs) vs side scatter (SSCs) of analyzed cells. PE-Ly6G positive cells were identified by analyzing FL2 vs FSCs plots. Unstained and isotype antibody stained samples were used to find non-specific fluorescence intensity. Data files were analyzed with FCS Express 4 flow cytometry software (DeNovo Software, Los Angeles, CA).

Bioluminescence signal

To determine whether activated neutrophils show a bioluminescence signal in the presence of luminol, neutrophils were collected from the mice according to [51]. In the

treatment group, 20,000 collected neutrophils were activated by phorbol myristate acetate (PMA, 2.5μM) and luminescence was measured after adding luminol (200 uM). PMA treated or luminol treated or untreated neutrophils were used as controls. The bioluminescence signal was monitored for 1 hour using an IVIS Lumina II imaging system (Caliper Life Sciences) and luminescence signal intensity was compared between different groups.

in vivo experiment

Mouse tumor model

9 week old female BALB/c mice were obtained from Charles River Laboratories, Wilmington, MA. Mice were maintained according to approved IACUC procedures (protocol 3060) in the Comparative Medicine Group facility of Kansas State University. Before 4T1 luc2 cell transplantation, fur was clipped on the ventral surface to identify mammary fat pads. $1X10^5$ 4T1luc2 cells in 25 μl phosphate buffered saline (PBS) were transplanted orthotopically into the fat pad of mammary gland number seven. Since the 4T1luc2 cell line expresses firefly luciferase, tumors can be identified by bioluminescent imaging after administration of D-luciferin. Control mice were injected with 25 μl phosphate buffered saline (PBS) orthotopically into mammary fat pad number seven.

Bioluminescence imaging

As a positive control, the light sensitive substrate D-luciferin (15mg/mL in 1X PBS) was given to the mice intraperitoneally at a dose of 150mg/kg. To demonstrate luminol-dependent bioluminescence, a three hour gap was allowed between D-luciferin and luminol injections. After that, mice were injected intraperitoneally with luminol (30mg/mL in water) at a dose of 300mg/kg. In both cases, mice were placed beneath the CCD camera in an IVIS Lumina II

imaging system and retained under isoflurane anesthesia (1.5%-2.0%) for the period of imaging. Bioluminescence was recorded 5 minutes after D-luciferin and luminol injections. For D-luciferin, mice were imaged on days 1, 2 and 3 after 4T1luc2 cells or PBS sham injection. For luminol, mice were imaged on days 1, 2, 3, 4, and 5 after 4T1luc2 cells or PBS sham injection. The area of 4T1luc2 cell or PBS injection (mammary pad 7) was selected as the region of interest (ROI) on bioluminescent images (Figure 2-5). Boundaries of the ROI were defined based on the luminescence signal in 4T1luc2 cell-injected mice, and the same size area was used in PBS-injected mice. The average radiance ($p/s/cm^2/sr$) from that ROI was used as the measurement for analysis. The duration of detectable bioluminescence occurring from firefly luciferase was found to be 30 minutes after luciferin administration. In order to avoid any potential overlap, we waited three hours after luciferin injection to administer luminol.

Luminol injection kinetics

To determine whether the luminol injection route affects luminescence peak signal time at the tumor site, two mice were injected intravenously with luminol (30mg/mL in water) at a dose of 300mg/kg. Two other mice were injected intraperitoneally with luminol (30mg/mL in water) at a dose of 300mg/kg. Both groups were placed beneath the CCD camera of the IVIS system and retained under isoflurane anesthesia (1.5%-2.0%) for the period of imaging *(*55 minutes). The area of 4T1luc2 cells or PBS injection (mammary pad 7) on bioluminescent images was selected as the region of interest (ROI). Boundaries of the ROI were defined based on the luminescence signal on 4T1luc2 cell-injected mice, and the same size area was used in PBS-injected mice. The average radiance ($p/s/cm^2/sr$) from that ROI was used as the measurement for analysis.

Statistical analysis

Statistical analysis was conducted using Winstat (A-Prompt Corporation, Lehigh Valley, PA) software and graphs were plotted in Microsoft Excel 2010. Dependent t-test was used to analyze differential count neutrophil percentages by taking the neutrophil percentage in WBCs as the measured variable. Repeated measures ANOVA was used to analyze *ex vivo* flow cytometry (percentage of gated cells as measured variable) and bioluminescence results (average radiance as measured variable), between groups significance was reported. p values less than 0.05 were considered as significant for the above analysis. *In vivo* D-luciferin imaging, luminol imaging, and luminol injection kinetics data were analyzed using repeated measures ANOVA by taking average radiance as measured variable; p values less than 0.05 were considered significant and between groups significance was reported. Non-significant results were interpreted cautiously based on the plotted graph trends. *In vivo* correlation between D-luciferin and luminol bioluminescence intensities was modeled by using simple linear regression and the coefficient of determination was reported.

Results

ex vivo

Differential count

One day after tumor cell transplantation, the neutrophil percentage in WBCs (Figure 2-2A) was normal [52]. However, on day 8 after tumor cell transplantation (Figure 2-2B), the neutrophil percentage in WBCs increased. The neutrophil percentage in WBCs in blood from mice on day 1 is significantly less than in blood from mice on day 8 (Figure 2-2C, p-value 0.01), demonstrating an increase in circulating neutrophils in 4T1luc2 tumor containing mice.

Flow cytometry

Samples of blood were collected from control and treatment groups at different time points. Results on day 3 after tumor cell transplantation showed no difference in percentage of Ly6G positive cells in WBCs between control mice and tumor-bearing mice. However, on days 6 and 12, the percentage of Ly6G positive cells in the control group was 9.84% and 14.40%; in the tumor-bearing mice, Ly6G positive cells increased to 34.26% and 65.89% (Figure 2-3A, B); the difference between groups is statistically significant (Figure 2-3C, repeated measures ANOVA p-value <0.05). These results indicate that tumor-bearing mice have increased circulating neutrophils compared with control mice.

Bioluminescence signal

PMA activated neutrophils showed bioluminescence signal after luminol addition (Figure 2-4A). Bioluminescence signal peak intensity was between 20-25 minutes after luminol addition and p-value of repeated measures between groups is less than 0.05 (Figure 2-4B).

in vivo

D-luciferin imaging

4T1luc2 cell-transplanted mice showed a bioluminescence signal at mammary fat pad number seven as early as day 1 with D-luciferin imaging (Figure 2-6A), suggesting that with D-luciferin imaging we can detect 4T1luc2 cells before they form palpable tumors. This finding is in agreement with the literature [29]. Note that luciferin bioimaging is used as a positive control for luminol imaging. Mice injected with PBS showed no bioluminescence signal with D-luciferin imaging (Figure 2-6A). D-luciferin imaging of mice on days 2 and 3 showed a bioluminescence signal at the 4T1luc2 cell injection site (Figure 2-6A); the intensity of

bioluminescence (average radiance) has an increasing trend over time (Figure 2-6B), indicating that at least during the early days following bioluminescent tumor cell transplantation, an increase in tumor size can be observed by D-luciferin imaging.

Luminol imaging

Bioluminescence imaging after luminol injection in mice showed a bioluminescence signal at the 4T1luc2 cell injection site (mammary fat pad number seven) on all imaged days starting from Day 1 (Figure 2-7A, red lines). Control mice injected with PBS showed weak signal at the injection site after luminol was administered on Day 1 but no signal on Day 2 (Figure 2-7A, blue lines). Apart from the tumor cell injection site, mice showed luminescence at other areas, primarily in the abdominal region. This may be because of peritonitis caused by intraperitoneal luminol injection. Also, some mice showed rectal light (Figure 2-7A) because luminol is known to be removed from the blood and excreted in the feces; this signal is likely due to this natural excretion. There were also small areas of signal in the neck-head region, probably due to skin nicking induced by clipping. Bioluminescence signal intensity from the injected area (mammary fat pad number seven) started increasing 2 days after 4T1luc2 cell transplantation, and over time, the signal intensity increased (Figure 2-7B). Also, D-luciferin and luminol bioluminescence intensities showed positive correlations on day 1($R^2 = 0.84$), day 2($R^2 = 0.83$) and day 3($R^2 = 0.82$) (Figure 2-7C).

Luminol injection kinetics

To see whether there is any difference in bioluminescence peak signal time at the 4T1luc2 cell injection site; mice were imaged after intravenous or intraperitoneal luminol injection. In both cases mice showed peak bioluminescence signal at the tumor area between five and 15 minutes after luminol injection (Figure 2-8A,B); the signal lasted for one hour after

the luminol injection. Consequently, intravenous injection of luminol resulted in the stronger bioluminescence signals. These results are in principal agreement with earlier imaging experiments in mice utilizing firefly luciferase [36, 53]. Since both luminol and luciferin are small molecules, it is not surprising that similar *in-vivo* kinetics are observed.

Discussion

The work described above demonstrates that orthotopically transplanted 4T1luc2 mammary adenocarcinoma cells can be successfully imaged by means of luminol-based bioluminescence imaging even before tumors are palpable. Although control mice injected with saline did show a small signal, the control bioluminescence signal disappeared after two days, in contrast to the transplanted tumor signal. Also, mice showed luminescence at other areas apart from the tumor cell injection site, primarily in the abdominal region. This may be because of peritonitis caused by intraperitoneal luminol injection. Skin nicks due to clipping also produced small signals in the neck and head region on days 1 and 2 after tumor cell inoculation. The intensity of the luminol-based BLI in mammary fat pad 7 increased over time after tumor transplantation. This is the first report of early tumor imaging of solid carcinomas using luminol alone in a preclinical model without additional components. Previously, luminol-based BLI was shown to be effective in early imaging in a transgenic preclinical model of a hematological cancer [43]. Zhang *et al.* studied the MPO dependence of the luminol bioluminescence signal [47]. When luminol was injected into MPO-positive mice and MPO-deficient mice, no luminescence signal was observed in the group of MPO-deficient mice. Based on these studies [43, 46], it is our paradigm that the luminol BLI signal we detected here is based on MPO activity released from activated neutrophils because of tumor transplantation [43].

The emission maximum of luminol-based bioluminescence is at λ= 425 nm [54]. At this wavelength, tissue penetration (decrease of the luminescence signal to 1/e) is estimated at 0.5 mm [55], corresponding to a tissue path length (99% light absorption) of approximately 2.2 mm. In conclusion, the penetration depth of luminol-based bioluminescence is not well suited for imaging deep-seated tumors [47]. Therefore, two principal strategies can be pursued for achieving enhanced bioluminescence signals. The first strategy comprises measures to enhance the photon flux of the light emitted at 425nm. It has been reported that β-cyclodextrin can enhance luminol luminescence [56]. Another study employed the chemiluminescent probe, L-012 (8-amino-5-chloro-7-phenylpyrido [3,4-d]pyridazine-1,4(2H,3H)dione), a substrate that has the potential of generating more light than luminol, for detecting MPO activity [57, 58]. The second strategy, described by Zhang *et al.*, uses NIR-emitting Q-dot nanoparticles, which absorb the luminol-based bioluminescence at 425 nm and reemit them as NIR photons [47]. It is noteworthy that the light penetration depth in the near infrared region is approximately 10 times larger than in the blue region of the visible spectrum [55]. The drawback of this strategy is that most nanoparticles of this type are cytotoxic [59]. Therefore, administering additional imaging agents, such as NIR-emitting nanoparticles may not be an option when imaging tumors in humans to observe their response to treatment. But, exploring additional measures of enhancing the luminescent signal may be useful for increasing the ability of luminol to detect deeper tumors.

It has been reported that the numbers of neutrophil granulocytes increase in the circulation in animals and humans with a variety of tumors [60]. Tumor cells secrete different cytokines and chemotactic factors which can cause recruitment and activation of neutrophils and other immune cells. Some examples are interleukins (IL-6 and IL-8) [61, 62], as well as

interferons (IFN-γ, INF-α, INF-β), and tumor necrosis factor-α (TNF-α)[63]. Furthermore, neutrophils are known to be a major component of inflammatory infiltrates in glioma [64], micropapillary carcinoma in the pancreas [65], human fibrosarcoma [66] , prostate carcinoma [67] and gastric carcinoma [68]. Also, it has been reported that neutrophils accumulate in the lungs before the arrival of metastatic cells in breast cancer models [52]. These studies, which demonstrate neutrophil infiltration in different types of tumors, suggest that luminol-based BLI detection of infiltrating neutrophils has potential for early human tumor detection.

Luminol has been used in humans for treatment of alopecia areata [69]; those studies showed it to be safe and rapidly excreted, with no toxic side effects observed. In conclusion, luminol or other luminescent substrates could potentially be used in human patients for imaging tumors. Although this study is a proof-of-principle, the method reported here could potentially be developed to screen for recurrence of other superficial cancers.

Figures

Figure 2-1 Neutrophil-mediated oxidation and chemiluminescence of luminol

(Phox: NADPH oxidase, SD: superoxide dismutase, MPO: myeloperoxidase)

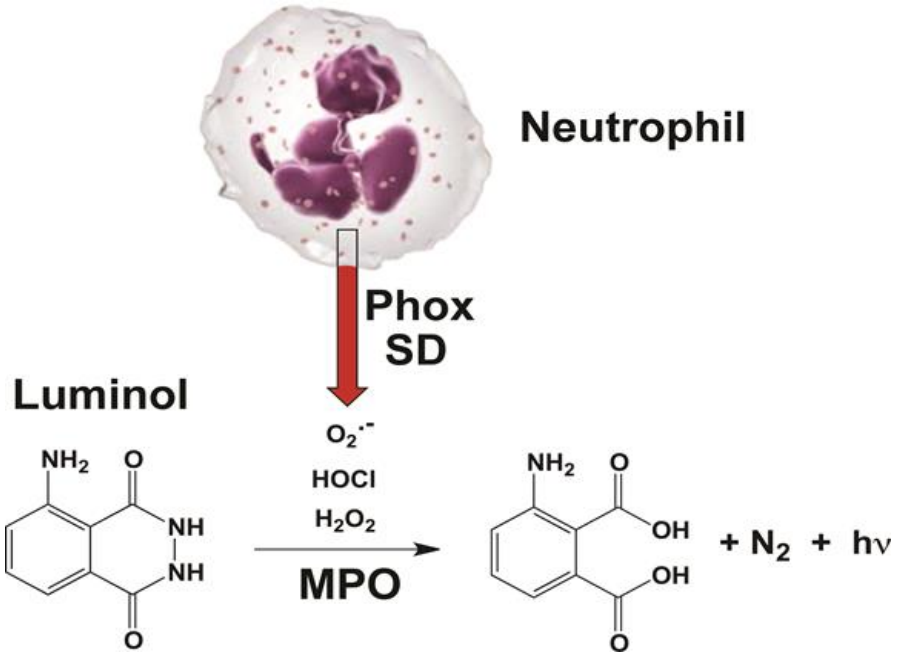

Figure 2-2 Differential count

A. Differential count of neutrophils on day 1 one after tumor cell transplantation was normal. **B**. Differential count of neutrophils on day 8 showed increased neutrophil percentage in WBCs. **C.** Comparison between days 1 and 8 demonstrated neutrophils percentage in WBCs increased in the circulation over time after tumor transplantation (p-value 0.01). All scale bars= 10µm; objective is 100x.

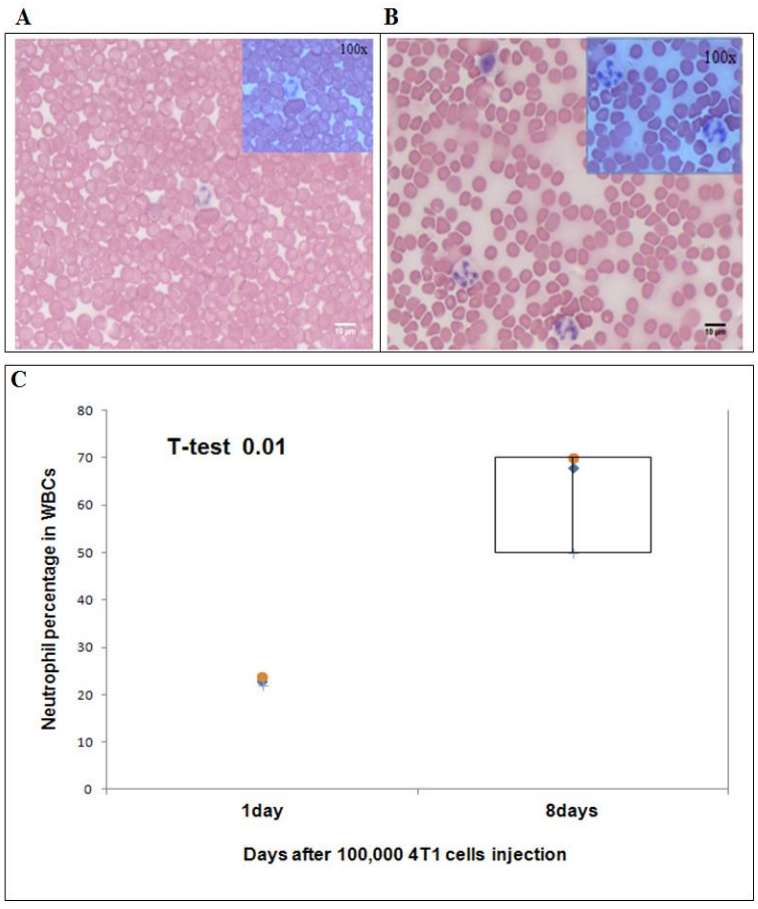

Figure 2-3 Flow cytometry

A. Normal mouse blood stained with Ly-6G or isotype at different time points on days 3, 6, 12 after tumor cell transplantation. Neutrophil percentages were determined on day 3 (13.23%), day 6 (9.84%), and day 12 (14.40%). **B.** Tumor-bearing mouse blood stained with Ly-6G. Neutrophil percentages were determined on day 3 (14.71%), day 6 (34.26%), and day 12 (65.89%). **C.** Graph indicates that tumor-bearing mice on days 6 and 12 showed increased neutrophils in WBCs circulation compared with other groups. The p-value of repeated measures between groups is <0.05.

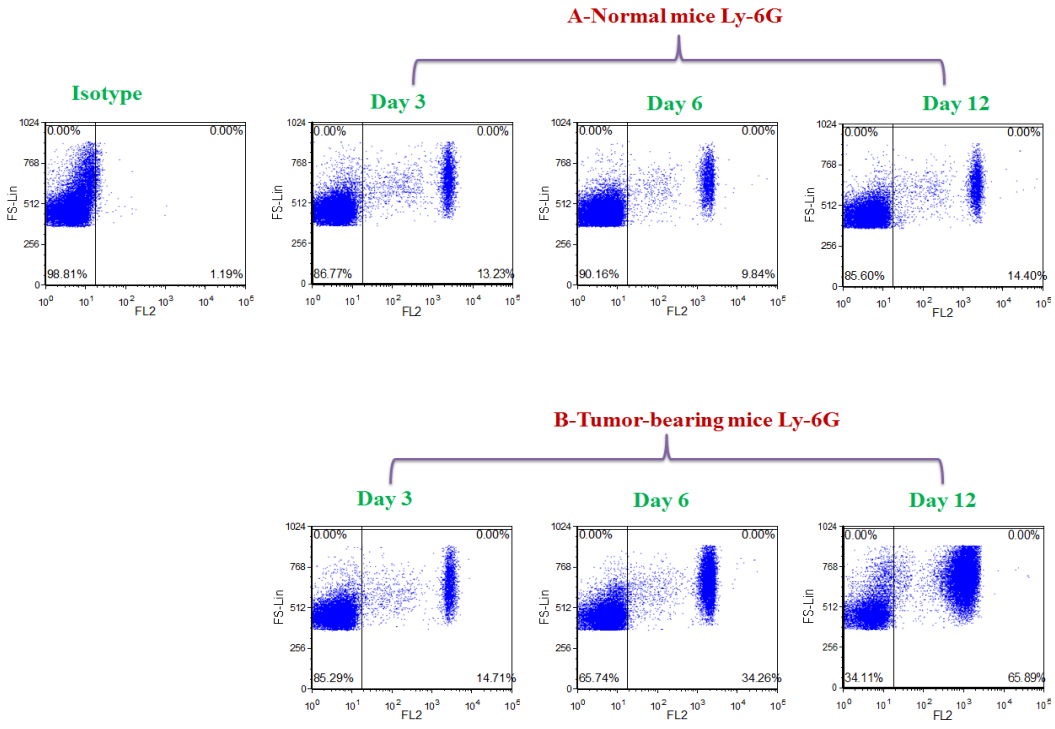

Figure 2-4 Bioluminescence signal in *ex vivo*

A. Neutrophils were placed in a 96-well assay plate. PMA (2.5μM), luminol (200 uM), or luminol+PMA were added to the cells. Activated neutrophils with PMA showed bioluminescence signal after luminol was added. **B.** Bioluminescence signal peak from Luminol+PMA group was between 20-25 minutes after neutrophil stimulation; the p-value of repeated measures between groups is <0.05.

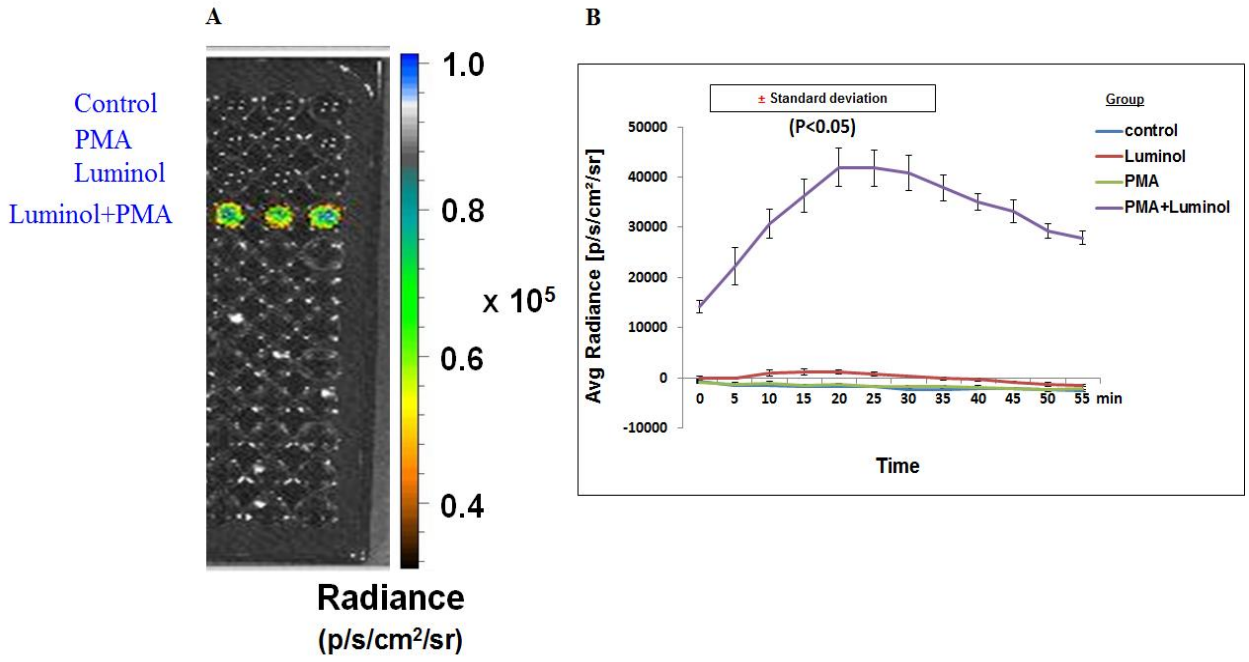

Figure 2-5 Bioluminescence measurement

Mammary pad number 7, the site of 4T1luc2 cell injection (red lines, left four mice) or PBS injection (blue lines, right two mice), was selected as the region of interest (ROI). The average radiance (p/s/cm^2/sr) from that ROI was used as measurement for analysis.

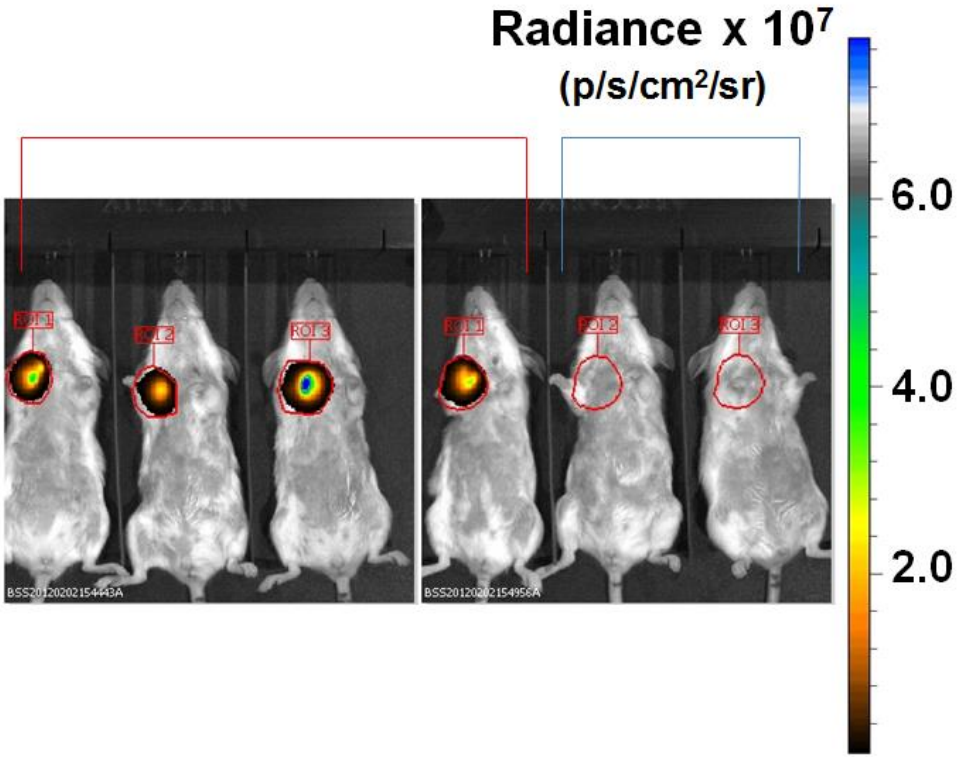

Figure 2-6 D-luciferin imaging

A. D-luciferin injections were given to the mice intraperitoneally on days 1, 2, and 3 after 4T1 luc2 cell injection. Red lines (left four mice): mice injected with 4T1 luc2 cells in mammary fat pad number seven. Blue lines (right two mice): control mice injected with PBS in mammary fat pad number seven. A luminescence signal was observable at mammary fat pad number seven as early as on day 1 when imaging with D-luciferin in 4T1 luc2 cells injected mice. **B**. Graph of the intensity of luminescence (average radiance, p/s/cm^2/sr) is showing an increasing trend from day 1 to day 3, suggesting that an increase in tumor size can be observed by D-luciferin imaging, as shown by previous studies [29]. The p-value of repeated measures between groups is <0.05.

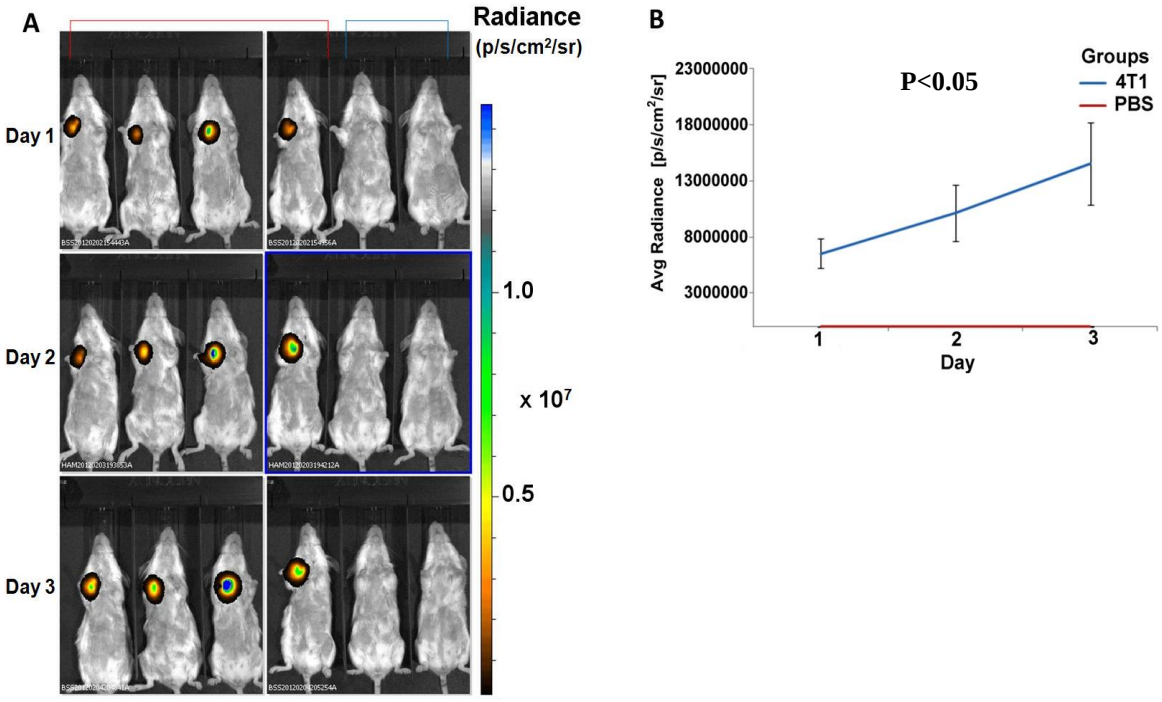

Figure 2-7 Luminol imaging

A. Luminol injections were given intraperitoneally to 4T1-bearing and control groups of mice on days 1 to 5 after 4T1luc2 cell injection or PBS injection. Red lines (left four mice): mice injected with 4T1luc2 cells. Blue lines (right two mice): control mice injected with PBS. Luminol signal was seen at the 4T1luc2 cell injection site (mammary fat pad number seven) on all the imaged days starting from day 1. PBS injected mice (right two mice) showed virtually no signal at mammary fat pad number seven, but showed signal mainly in the abdominal region. **B**. Bioluminescence signal intensity (average radiance (p/s/cm^2/sr) at mammary fat pad number seven increased by 3 days after 4T1luc2 cell transplantation, and over time, the signal intensity increased. The p-value of repeated measures between groups is <0.05. **C.** Comparison of D-luciferin and luminol bioluminescence intensities showed positive correlation for day 1(R^2-0.84), day 2(R^2-.83) and day 3(R^2-0.82).

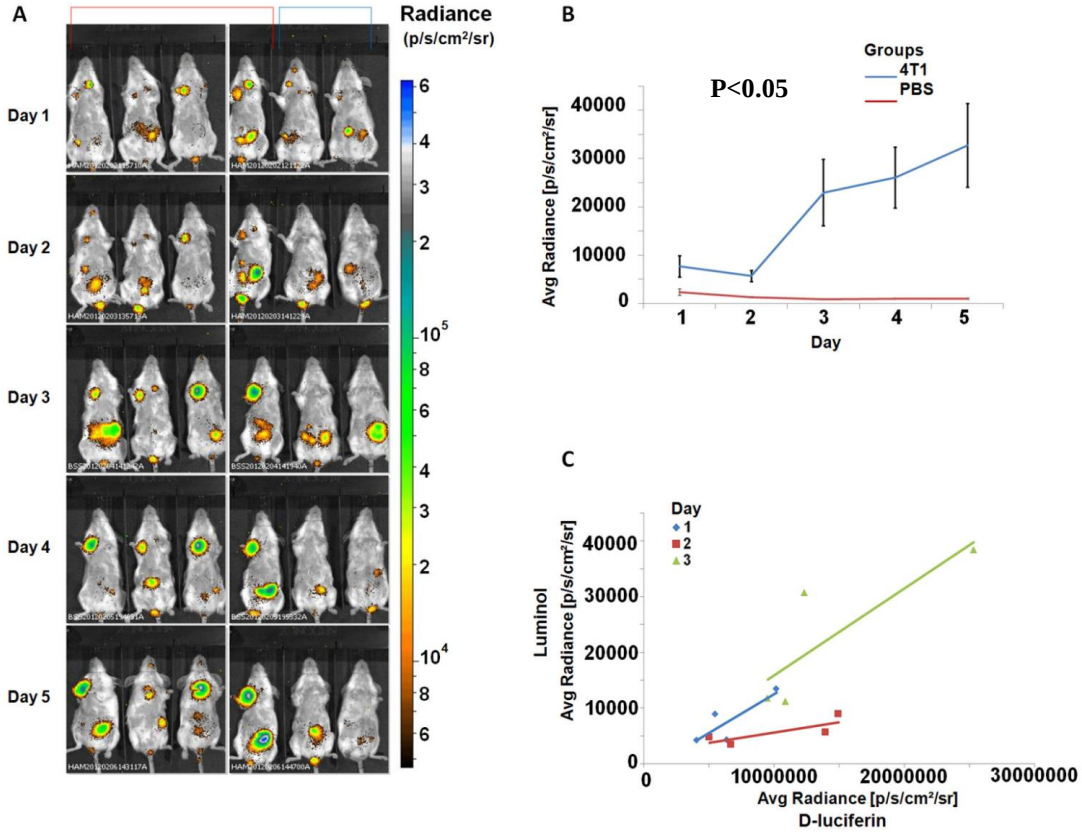

Figure 2-8 Luminol injection kinetics

A. Comparison of intravenous (two mice, right) and intraperitoneal (two mice, left) luminol injections to observe the difference in bioluminescence peak signal time at the 4T1luc2 cell injection site. Mice were imaged every 10 minutes with an accumulation time of 5 minutes, resulting in a total imaging time of 55 min. after luminol injections. Luminescence peaked between 5 and 15 minutes regardless of injection method. **B.** Graph showing the bioluminescence signal (average radiance, p/s/cm^2/sr) intensity after intraperitoneal and intravenous administration.

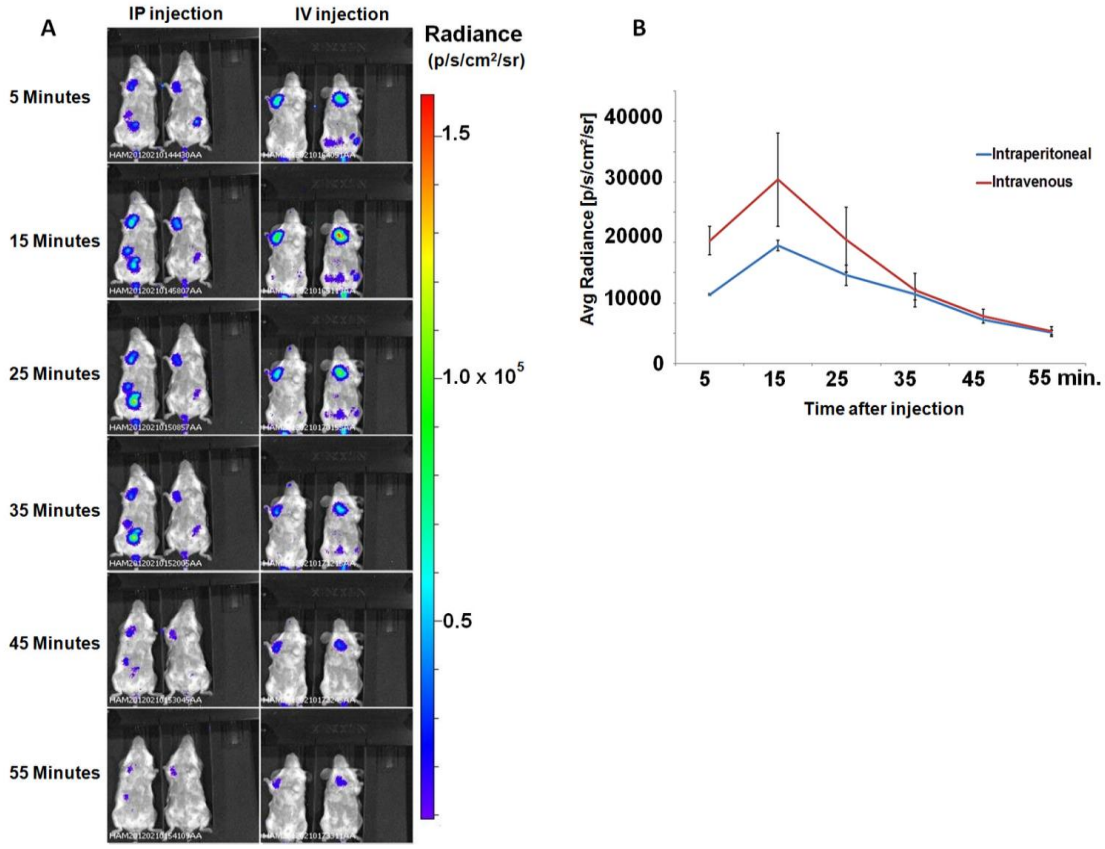

Chapter 3 - Luminol-based *in situ* photodynamic therapy for pre-clinical breast adenocarcinoma

Based on work to be submitted for publication with authors shown below:

Hamad S. Alshetaiwi*[a], Tej B. Shrestha*[a], Sivasai Balivada[a], Matthew T. Basel[a], Marla Pyle[a], Thilani N Samarakoon[b], Hongwang Wang[b], Dipak Giri[b], Daniel Higgins[b], Stefan H. Bossmann[b], Deryl L. Troyer[a]

*These two authors contributed equally to this work and are co-first authors.

[a] Department of Anatomy and Physiology, Kansas State University, Manhattan, KS 66506, USA

[b] Department of Chemistry, Kansas State University, Manhattan, KS 66506, USA

Abstract

Photodynamic therapy (PDT) is a cancer treatment that uses a photosensitizer and a specific wavelength of light. When tumor cells which have absorbed the photosensitizer are exposed to the correct wavelength of light, reactive oxygen species are generated, resulting in tumor cell death. Poor tissue penetration of light is a major limitation in PDT, restricting its use to treatment of localized tumors. Light generation at the tumor area might increase the effectiveness of PDT and could expand its use for metastatic tumors. Infiltration of tumor-activated polymorphonuclear neutrophils (PMNs) produces luminescence in the presence of luminol; this bioluminescence has been used for tumor detection in pre-clinical trials [10, 43]. Based on this rationale, we hypothesized that luminol-based bioluminescence can cause targeted PDT in breast adenocarcinoma tumors in the presence of the photosensitizer 5-aminolevulinic acid (ALA). To test this hypothesis, BALB/c mice were transplanted with 4T1luc2 mammary adenocarcinoma cells to establish a breast adenocarcinoma model. After tumor formation, ALA and luminol were administered to mice through intraperitoneal and intravenous routes, respectively. This treatment regimen was repeated six times and ALA alone/luminol alone/saline treated tumor-bearing mice were used as controls. Relative differences in the increase of tumor volume and final tumor weights were analyzed to test the treatment hypothesis. Analysis of the data showed that luminol treatments resulted in breast adenocarcinoma tumor growth attenuation. This study gives evidence for the antitumor activity of luminol on breast adenocarcinoma, possibly through *in situ* PDT.

Introduction

Light has been considered as a treatment of various diseases, including skin cancer, for more than three thousand years [17]. In the 19th century, Niels Finesen used light to prevent the formation of smallpox pustules [70]. Then, in 1903, a skin tumor was treated by applying eosin and using white light [71]. These treatments led to the first introduction of the term 'photodynamic therapy (PDT)' in 1907. It is defined as the therapeutic use of non-toxic photosensitizers and harmless light in combination with oxygen [17]. The mechanism of PDT starts when tumor cells which have absorbed a photosensitizer are exposed to the correct wavelength of light to excite the photosensitizer from its ground state (S0) to the first singlet state (S1) and then to first excited triplet state (T1) [17]. This excited triplet state of the photosensitizer can undergo two kinds of reactions. For the type 1 reaction, the excited triplet can react directly with a cell membrane or a molecule which can transfer an electron or hydrogen atom to produce free radicals [72]. Thus, these free radicals react with oxygen to generate reactive oxygen species (ROS) such as superoxide anions or hydroxyl radicals, resulting in tumor cell death [72]. On the other hand, in type 2 reactions, the triplet state can transfer its energy to molecular oxygen to form singlet oxygen, which can cause oxidative damage in target cells [72].

It has been reported that PDT can mediate tumor destruction by three different strategies [15]. First, ROS can cause direct tumor cell destruction. ROS can induce lipid peroxidation in the cell wall and that leads to modification of some proteins which may cause DNA damage [73]. Additionally, ROS can disrupt the mitochondrial membrane, resulting in cytochrome c release into the cytosol which can activate caspases, causing apoptosis [74]. The second strategy of PDT is vascular damage. It has been known that viability of tumor cells depends on the nutrients that have been provided by the blood vessels [17]. Therefore, targeting tumor

vasculature is one promising approach for cancer therapy. Dennis *et al*. have demonstrated that treated breast tumors showed vascular disruption, necrosis and white blood cell (WBC) infiltration after three days of PDT [75]. The third strategy of PDT is activation of immune response. This is in contrast to most common cancer treatments, which are immunosuppressive [15]. Present cancer therapies, like chemotherapy and radiation, target quickly dividing cells [12, 13]. Therefore, these therapies damage some fast-dividing normal progenitor cells, for example, cells lining the digestive tract and hematopoietic stem cells [14]. Some of the side effects of chemotherapy and radiation therapy are due to their effect on these normal cells. Also, high doses of chemotherapy and radiation therapy are toxic to the bone marrow, which is the source of immune cells [15].

Clearly, the main goal of cancer therapy today should be not only to kill tumor cells but at the same time to activate the immune system to identify and terminate any remaining tumor cells [15]. Therefore, different research teams are trying to develop a variety of targeting treatments which might have these desirable properties. PDT is one example of this [15]. Several studies have shown that PDT can cause an inflammatory response and several cytokines can be released, for instance interleukins (IL-1β, IL-6, IL-8, IL-10) and tumor necrosis factor-α (TNF-α), which can recruit immune cells such as dendritic cells, neutrophils, macrophages and lymphocytes [15, 76].

Therefore, to accomplish PDT there are some requirements of photosensitizers such as selectivity to tumor cells, fast tumor accumulation, no toxicity in the absence of light, high absorption and activation by light with good tissue penetration [74]. Different research groups reported that there are several mechanisms to retain photosensitizers within tumors. High expression of low density lipoprotein receptor (LDL) on cancer cells has the ability to bind to

many photosensitizers like porphyrins [77]. Low pH in tumor cells increases cellular uptake of photosensitizers and increases vascular permeability [74]. Moreover, decreased activity of ferrochelatase in cancer cells may cause a photosensitizer like ALA to accumulate in more in cancer cells than in normal cells [78]. Different studies showed that targeted knockdown of ferrochelatase [79] and pre-treatment of tumor cells with ferrochelatase inhibitors [80] have improved ALA-PDT outcome. There are a variety of photosensitizers that have been examined for PDT such as ALA, benzoporphyrin, Foscan and Photofrin [72, 78].

ALA is an endogenous amino acid which is a precursor of the photosensitizer protoporphyrin IX (PpIX), which is normally formed in the mitochondria. Tumor cells metabolize ALA into PpIX [78, 81]. ALA is a non-toxic compound and different studies demonstrated that ALA administration with light exposure could inhibit the growth of a variety of tumor models [82]. Examples include pancreatic tumors [83], colonic tumors [84], mammary carcinoma/adenocarcinoma [85, 86] and skin tumors such as basal cell carcinomas and squamous cells carcinomas [76, 82] .

Although many research groups are working to improve PDT, it still has limitations. One of the main concerns in PDT is light delivery and distribution in tissues [87]. It has been reported that light penetration in tissue decreases exponentially with distance. Even with longer wavelengths, light penetrates on average of 1-3mm [87]. Liver has poor light penetration because it has high hemoglobin content. Also, brain tissue will cause light scattering [87]. Subsequently, these drawbacks in PDT restrict its use to treatment of localized and superficial tumors. Based on this background information, we wondered whether light generation at the tumor area could increase the effectiveness of PDT and potentially expand its use for deep and/or metastatic tumors. Our previous study demonstrated that infiltration of tumor-activated

polymorphonuclear neutrophils (PMNs) in a breast adenocarcinoma model produces luminescence in the presence of luminol; this bioluminescence has been used for tumor detection in pre-clinical trials [10]. Therefore, luminol could potentially be used as an in *situ* light source to trigger the photosensitizer. Based on this rationale, we hypothesized that luminol-based bioluminescence can cause targeted PDT in breast adenocarcinoma tumors in the presence of the ALA.

Material and Methods

Chemicals and Reagents

5-aminolevulinic acid hydrochloride was purchased from Sigma Aldrich, Saint Louis, Missouri. Luminol sodium salt was obtained from Santa Cruz Biotechnology, (Santa Cruz, California. Bovine serum albumin (BSA) was acquired from Sigma-Aldrich. DeadEnd^{TM} Colorimetric TUNEL System kit was from Promega, Madison, WI. CD49b primary antibody, a rabbit monoclonal antibody, was obtained from Novus Biologicals, Littleton, CO. Secondary antibody goat anti-rabbit IgG Alex Fluor 568 (2mg/ml) was purchased from Molecular Probes (Life Technologies), Grand Island, NY. Normal goat serum (NGS) was from RDI Fitzgerald, Acton, MA. Tris and NaCl were acquired from Fisher Scientific, Waltham, MA. Triton X-100 was from Sigma-Aldrich, St. Louis, MO. Fluoromount-G^{TM}, was from Southern Biotech, Birmingham, AL

Cell Culture and Mouse tumor model

Mouse mammary gland adenocarcinoma tumor cells expressing firefly luciferase (4T1luc2) were obtained from Caliper Life Sciences, Hopkinton, MA [50]. Cells were

maintained in RPMI1640 medium supplemented with 1% penicillin/ streptomycin (Invitrogen, Grand Island, NY) and 10% fetal bovine serum (FBS; Sigma-Aldrich, St. Louis, MO). Cells were incubated at 37°C and 5% CO_2. 9 week old female BALB/c mice were purchased from Charles River Laboratories, Wilmington, MA. Mice were used according to guidelines of Institutional Anima Care and Use Committee (IACUC) at the Comparative Medicine Group facility of Kansas State University.

In vivo experiment

Light generated by neutrophils in the presence of luminol and ALA was identified as main factors for experimental design based on our proposed hypothesis. Four separate animal experiments were conducted to test the primary hypothesis that luminol-generated light and ALA will interact with each other and decrease the 4T1luc2 tumor burden. The design for each experiment was progressively modified based on the findings from previous experiment(s). The first three studies were used as exploratory and the final study was used as confirmatory. On day 0 of the first experiment, 28 mice received orthotopic transplants of $1X10^5$ 4T1luc2 cells in 10 µl phosphate buffered saline (PBS) into the fat pad of mammary gland number seven. On day 3 after tumor cell transplantation, mice were randomly divided into four groups with seven mice in each group: Group I- saline; Group II- ALA; Group III- luminol; and Group IV- ALA and luminol. Group -IV mice were injected with ALA (15 mg/ml in saline) at a dose of 150 mg/kg followed 4 hours later by intraperitoneal injection of luminol (30 mg/ml in saline) at a dose of 300 mg/kg on days 4, 6, 8, 10, and 12 after tumor cell transplantation. At the same time, Group I mice were injected with 200 ul of Saline, Group II mice were injected with ALA alone and Group III mice were injected with luminol alone. Tumor diameters were measured with a caliper on days 5, 7, 9, 11, and 13 (See Figure 3-1) and tumor volume was calculated by the formula $\pi/6$

*W^2L by assuming tumor is ellipsoid in shape. The shorter diameter was considered as width (W) and longer diameter was considered as length (L). All the mice were euthanized on day 13 and tumor weights were measured. Other organs were collected for further analysis.

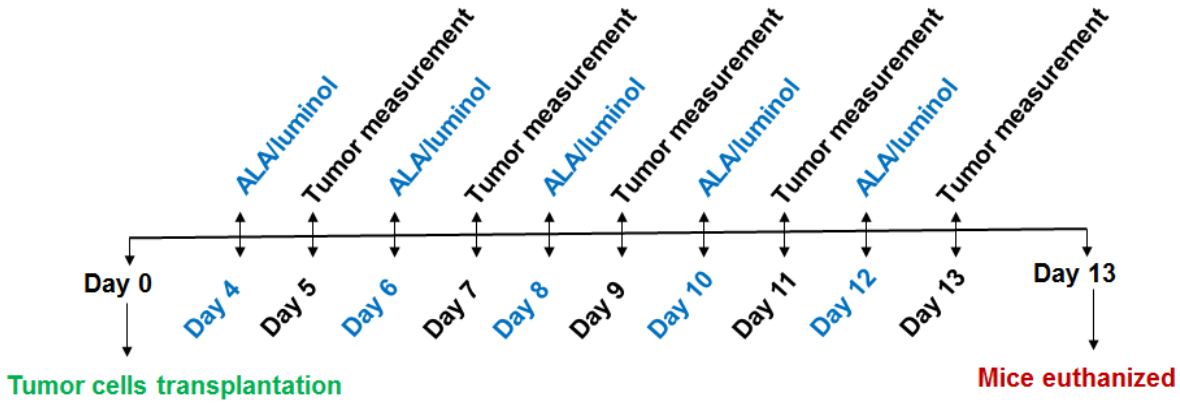

Figure 3-1 Treatment plan

Mice were treated on days 4, 6, 8, 10, and 12. Tumor sizes were measured with a caliper on day 5, 7, 9, 11, and 13. Mice were euthanized on day 13.

The second experiment was designed for slower tumor growth to allow more treatments. On day 0, $1X10^4$ 4T1luc2 cells were transplanted to 28 mice divided into four groups as explained above. Mice were treated on days 7, 10, 13, 16, 19, and 22 with the same doses described above in the first experiment. Tumors were measured on days 9, 11, 13, 15, 17, 19 and 21; volumes were calculated. All the mice were euthanized on day 23 and tumor weights were measured. Other organs were collected for further analysis.

In the third experiment, the route of luminol injections was changed from intraperitoneal to intravenous; also, the ALA dose was increased to 200 mg/kg (20 mg/ml in saline), the full treatment was compared to vehicle only, and the sample size was increased. On day 0 $1X10^4$

4T1luc2 cells were transplanted to 31 mice. On day 2 mice were divided randomly into two groups: Group I, control (saline) containing fifteen mice, and Group II, ALA/luminol (treatment) containing sixteen mice. On days 4, 7, 10, 13, 16, and 19, Group II mice received intraperitoneal ALA injection followed 4 hours later by intravenous luminol injection. Group I mice received saline at the same time. Tumors were measured on days 7, 9, 11, 13, 15, 17, 19, 20, and 21 (See Figure 3-2). Tumor volume was calculated as explained above and mice were euthanized on day 21. Tumors were collected, weights measured and other organs were collected for further analysis.

The final and fourth experiment was designed by considering information from all the previous three experiments with increased sample size. Sixty four mice were transplanted with $1X10^4$ 4T1luc2 cells on day 0. On day 2, mice were randomly divided into the following groups; Group I- saline, Group II- ALA, Group III- luminol, and Group IV- ALA & luminol. Mice were treated on days 4, 7, 10, 13, 16, and 19 with the same doses that are described above in the third experiment. Tumors were measured on days 7, 9, 11, 13, 15, 17 and 19 and tumor volumes were calculated. All the mice were euthanized on day 21. Tumor tissues and other organs were collected for further analysis.

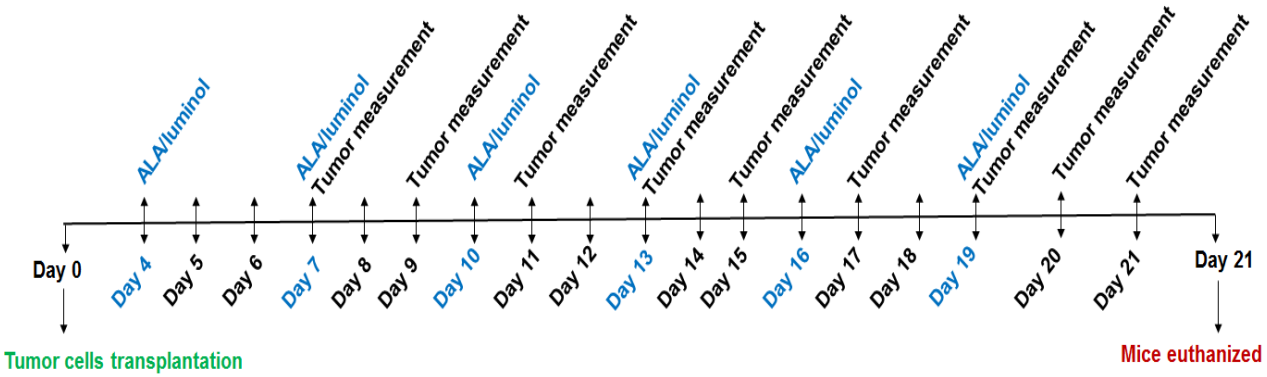

Figure 3-2 Treatment plan

Mice were treated on days 4, 7, 10, 13, 16, and 19. Tumors were measured with a caliper on days 7, 9, 11, 13, 15, 17, 19, 20, and 21. Mice were euthanized on day 21.

Apoptosis assay

After mice were euthanized, tumors were snap-frozen in liquid nitrogen for histological analysis. Tumors were sectioned on a cryostat (Leitz Kryostat 1720, Germany) at 8−10 μm to be used for TUNEL assay, which labels the fragmented DNA of apoptotic cells. Apoptotic cell detection was performed on tumor sections according to the DeadEnd^{TM} Colorimetric TUNEL System protocol [88]. Briefly, sections were fixed with 10% buffered neutral formalin. Then, sections were permeabilized with proteinase K. Biotinylated nucleotide was mixed on ice with recombinant terminal deoxynucleotidyl transferase (rTdT) enzyme and incubated on the sections for 60 minutes. For blocking, slides were immersed in 0.3% hydrogen peroxide for 5minutes. Then, horseradish peroxidase-labeled streptavidin (HRP) was added to the slides. Additionally, slides were stained with the chromogen diaminobenzidine (DAB) followed by nuclear counterstain (methyl green).

Immunohistochemistry

Tumor tissues were snap-frozen and sectioned as described above. CD49b is specific for natural killer cells (NK). Samples were prepared for CD49b and incubated for 5 minutes in 0.025%Triton X-100 in TBS. To prevent non-specific binding of immunoglobulins, sections were incubated for 1hour at room temperature with 10%NGS, 1%BSA in 1xTBS. After blocking, primary antibody was added to the sections at a dilution of 1:500 and incubated overnight in the dark at 4°C. After incubation, sections were washed for 5 minutes with 0.025%Triton X-100 in TBS. Then, secondary antibody was added at a 1:500 dilution and incubated for 1hour at 37°C. Finally, samples were stained with Hoechst, 10µg/ml, for 15minutes and mounted in Fluoromount-G.

Statistical analysis

Statistical analysis was conducted using SAS V8 software and graphs were plotted in Microsoft Excel 2010. In all the reported graphs standard error of the mean was used for error bars. *In vivo* experiments were designed following fixed effects, balanced, completely randomized 2X2 factorial design with luminol and ALA as treatment factors and with tumor volume and weights as response variables. Tumor volume measurements were analyzed using univariate fixed effects repeated measures two way ANOVA and tumor weight measurements were analyzed by using fixed effects two way ANOVA. Single factor experiments were analyzed by using repeated measures one way ANOVA in WinSTAT sofware (A-prompt Corporation, Lehigh Valley, PA). A p-value less than 0.05 was considered as significant for all statistical tests.

Results

In the first experiment, mice were treated four days after tumor cell transplantation. First, the photosensitizer ALA was injected intraperitoneally into the mice. Based on literature reports, ALA is known to accumulate at tumor site within 4 hours after injection. So, mice were injected intraperitoneally with luminol 4 hours after ALA administration to generate light at the tumor site. To identify differences in tumor growth patterns between groups, tumor volumes and weights were plotted and shown (Figure 3-3A&B). Analysis of tumor measurements demonstrated that luminol caused a significant effect on tumor growth (p-value <0.05 for both volumes and weights) and further, administration of ALA has no effect. Although this effect of luminol was surprising to us in the present study, a luminol-like compound, galavit, has been used previously as an immunomodulator [89-91].

Consequently, we thought about different strategies that might improve our treatment approach. It was decided to repeat this experiment with an increased number of treatments. The numbers of 4T1 cells transplanted were decreased to $1X10^4$ from $1X10^5$ 4T1luc2 cells to slow tumor growth and allow an increased number of treatments. Analysis of tumor volumes from this second experiment again gave evidence to the effect of luminol (Figure 3-4A) (p-value <0.05), similar to the first experiment. But tumor weight analysis showed no statistically significant results to any of the expected effect (Figure 3-4B); however, this could be due to loss of mass due to extensive necrosis in larger tumors or insufficient sample size.

Based on these results from two experiments, we decided to repeat the experiment for the third time with more modifications. The number of mice in the saline control group was increased to fifteen and in the treatment group (ALA/Luminol) was increased to sixteen. Additionally, the route of luminol injections was changed to intravenous because in our previous

study, mice with intraperitoneal injection showed luminescence in the abdominal [10]. Also, the dose of ALA was increased to 200 mg/kg. The number of 4T1 cells transplanted was the same as for the second experiment.

In the third experiment, we only used two groups, saline versus luminol and ALA treatment. We found in this experiment that there was a substantial delay in mammary adenocarcinoma tumor growth in the treatment group (p-value <0.05) (Figure 3-5A). On day 21 mice were euthanized and tumor weights were measured. Results indicated there was difference between the groups (p-value <0.05) (Figure 3-5B).

Accordingly, we decided to conduct the final confirmatory experiment with all the groups (saline, ALA, luminol and ALA/luminol) and followed the same methods that we used in the third experiment. Analysis of the data showed that treatment with a combination of luminol and ALA as well as treatment with luminol alone resulted in breast adenocarcinoma tumor growth attenuation (Figures 3-6A&B), and luminol had a significant effect on tumor size (p-value <0.05 for tumor volume and mass). These results indicated there is an antitumor activity of luminol on breast adenocarcinoma.

Histological and immunohistochemical analysis

To discern potential mechanisms of tumor attenuation, we performed histological examination. Tumor sections in all groups were stained with a DeadEnd^{TM} Colorimetric TUNEL System kit to identify the degree of apoptosis. The histological findings of the apoptosis assay indicated a qualitative difference between the groups. Based on our observation we could see more positive apoptotic cells in luminol/ALA and luminol groups compared with other groups (Figure 3-7). Finally, we examined whether treatments altered natural killer cell (NK) infiltration to the tumor site. Immunohistochemistry for NK cells (CD49b) was performed in all

the groups (Figure 3-8). Results demonstrated there is qualitative difference between the groups, with. luminol/ALA and luminol groups appearing to have more NK cells compared to other groups.

Discussion

The studies described above resulted in the following findings. Luminol caused a decrease in 4T1 breast adenocarcinoma tumor growth, and ALA addition didn't change luminol's effect (Figure 3-6A&B). Histological and immunohistochemical examination showed increased apoptosis positive cells in luminol-treated groups compared with other groups (Figure 3-5, qualitative observation). Moreover, luminol-treated groups showed more NK cells compared with other groups (Figure 3-8, qualitative observation). We believe the possible mechanism for the luminol effect observed in the present study is through *in situ* PDT.

It is known that tumor cells have decreased activity of heme oxygenase and hence naturally accumulate protoporhyrin IX to a greater extent than normal cells [78]. Alternatively, other porphyrins could accumulate to a greater extent in tumor cells than in normal cells due to increased numbers of LDL receptors [77]. Endogenous porphyrins have been used as tumor imaging and photosensitizing agents [92]. We identifiedthat 4T1 luc2 tumors have increased amount of porphyrins compared with other tissues (data in Appendix A). When we tested luminol directly on 4T1 luc2 cells *in vitro*, we didn't see any cytotoxic effect (data in Appendix B), suggesting that the antitumor effect we observed on 4T1 tumors is not luminol's direct effect. Chen *et al*. also observed no luminol-mediated cytotoxic effect *in vitro* using a colon carcinoma cell [40]. However, Laptev *et al*. showed that luminol has direct cytotoxicity on Friend's leukemia cells *in vitro* [93]. Compared with 4T1 breast cancer cells, leukemia cells might have

increased capability of generating light in the presence of luminol *via* myeloperoxidase production.

The elimination of the need for photosensitizer could be advantageous in several ways. First, animal (or patient) discomfort or local tissue damage due to intravenous injections could be reduced. Second, the undesirable side effect of photosensitization due to systemically circulating photosensitizers could be reduced or eliminated.

Several strategies might increase the specificity and efficiency of PDT after our study. First, it has been reported that β-cyclodextrin could be used to enhance luminol luminescence [56]. Alternatively, utilizing delivery systems such as monoclonal antibodies, liposomes and nanoparticles as carriers for luminol might improve the selectivity to tumor site. Also, it might be possible to enhance PpIX accumulation in cancer cells. For instance, administration of low-doses of methotrexate three days prior to ALA-PDT showed enhancement of PpIX accumulation within skin carcinoma cells *in vitro* [94] and prostate cancer cells [95]. Furthermore, it has been shown that administration of vitamin D3 in squamous skin cancer mouse models prior to ALA administration increased PpIX accumulation and the efficiency of ALA-PDT with no toxic side effects [96].

PDT has shown variable results for some types of tumors in the clinic. For example, it has been used to treat patients with lung cancer [97], esophageal cancer [98] and gastric carcinoma [99] with encouraging results especially if treatment was initiated at an early stage. On the other hand, some clinical studies showed a limited effect for patients with brain tumors [100], head and neck tumors [101], colorectal cancer [102], breast cancer [103] and pancreatic cancer [104] due to the light delivery restrictions described in the introduction [17].

The method that we described here might allow PDT of deep or disseminated tumors to increase light delivery at deep sites that otherwise would be inaccessible. Several *in vitro* studies showed that luminol-based chemiluminescence could activate photodynamic destruction of cancer cells [93] [105]. R Laptev *et al.* have demonstrated that *in vitro* luminol activates bioconjugates composed of transferrin and hematoporphyrin to reduce numbers of tumor cells [93]. Bioluminescence resonance energy transfer (BRET), which involves a transfer of energy from a bioluminescence donor to a suitable acceptor molecule, has been used as an internal light source for PDT [106]. Lai *et al.* have developed a PDT system by using *Renilla luciferase*-immobilized quantum dots-655 (QD-RLuc8) as an internal light source to activate the photosensitizers and mediate PDT. However, QD have a cytotoxic effect, so using QD-RLuc8 to increase light source for PDT, may not be an option when treating tumors [106].

Luminol alone has been used in humans as treatment for alopecia areata with no toxic side effects observed [69]. In addition, Galavit, is monosodium compound (5-amino-2-3-dihydro-1-4-phthalazine dione) which is similar to luminol sodium salt, has shown some immunomodulatory effects in humans [89-91]. In clinical trials Larina *et al.* examined immune status after giving Galavit to 28 patients with cicatricial stenosis of the trachea. Results showed an increase in the numbers of natural killer cells (CD16+), T-helper cells (CD4+) and an induction of the phagocyte activity of neutrophils [89].

In conclusion, this study showed that it may be possible to target cancer cells by using luminol *in situ* PDT to produce light and destroy tumor cells in a preclinical model of breast adenocarcinoma. By developing this approach it might be possible to target photodynamic therapy to treat deep seated tumors that external light sources cannot reach.

Figures

Figure 3-3 Effect on tumor growth from experiment one

A. Calculated tumor volume comparison between different groups from day 5 to day 13. Luminol group demonstrated a significant effect on tumor growth. Data were analyzed using repeated measures two way ANOVA. **B.** Tumor mass comparison between different groups on day 13; luminol has a significant effect. Data were analyzed using two way ANOVA.

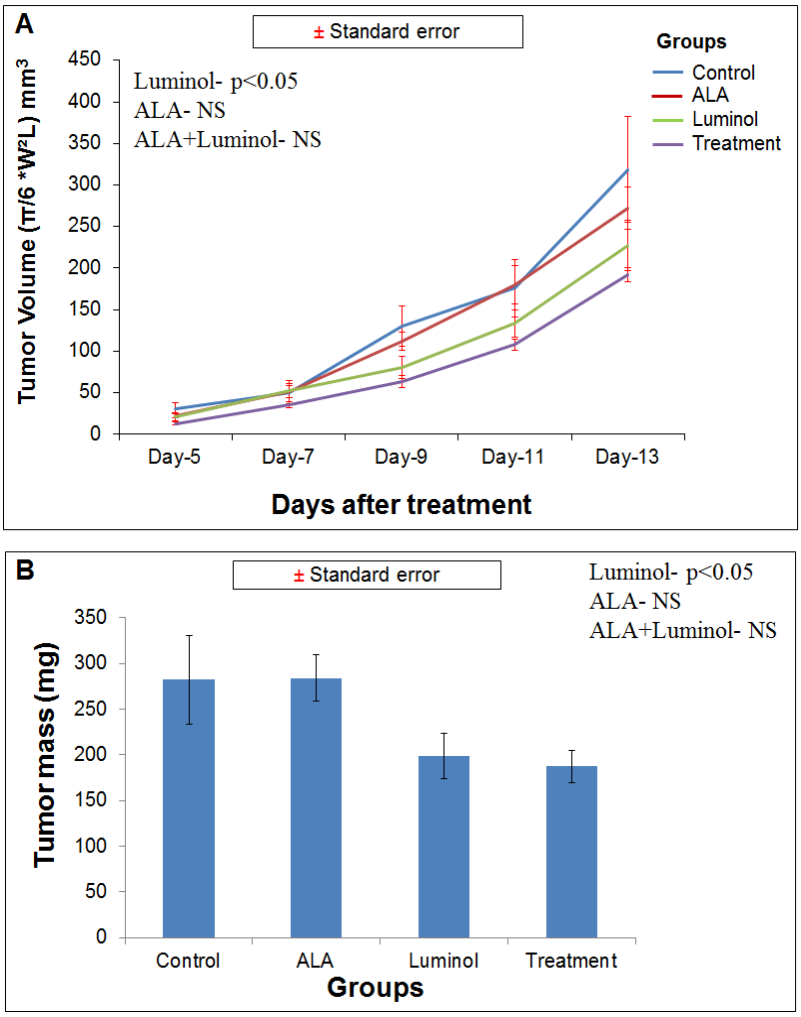

Figure 3-4 Effect on tumor growth from second experiment

A. Calculated tumor volume comparison between different groups from day 9 to day 21. Luminol group indicated a significant effect on tumor growth. Data were analyzed by using repeated measures two way ANOVA **B.** Tumor mass comparison between different groups on day-21;data were analyzed by using two way ANOVA (not significant).

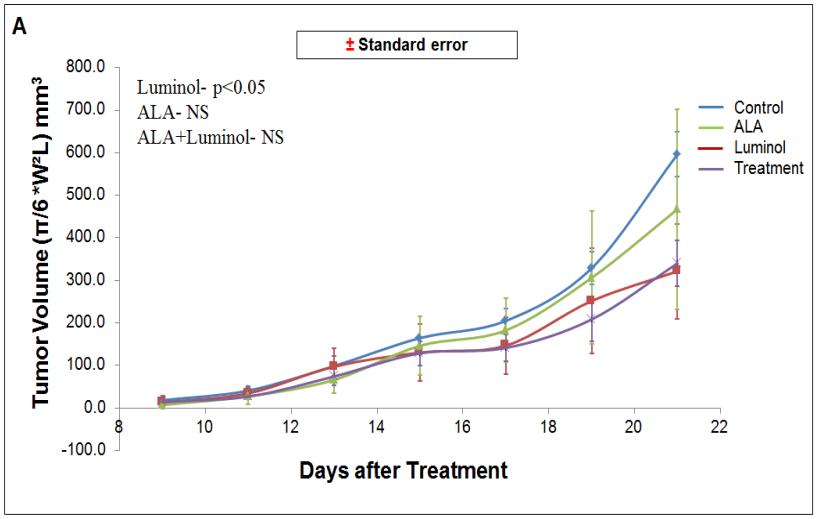

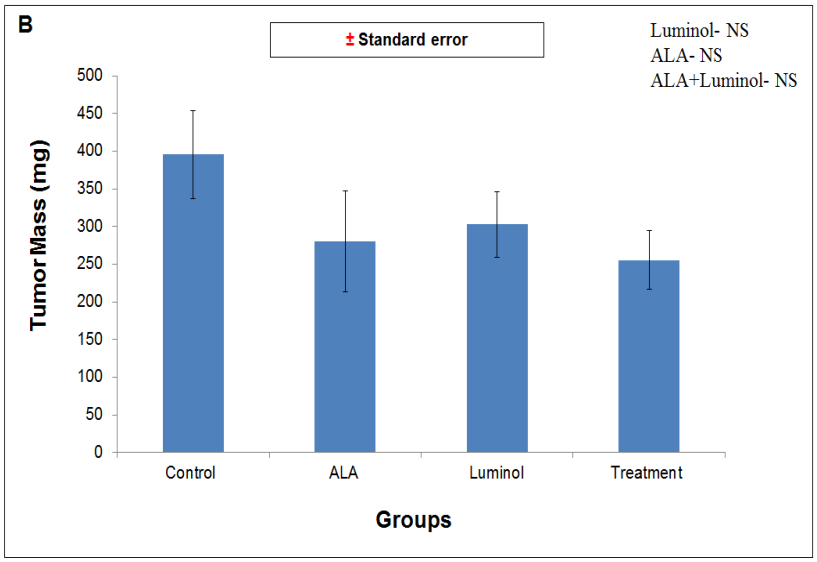

Figure 3-5 Effect on tumor growth from third experiment

A. Calculated tumor volume comparison between different groups from day 9 to day 21. Treatment group indicated a significant effect on tumor growth. Data were analyzed using repeated measures one way ANOVA (*p*-value <0.05). **B.** Tumor mass comparison between different groups on day-21, data were analyzed using t-test (*p*-value <0.05).

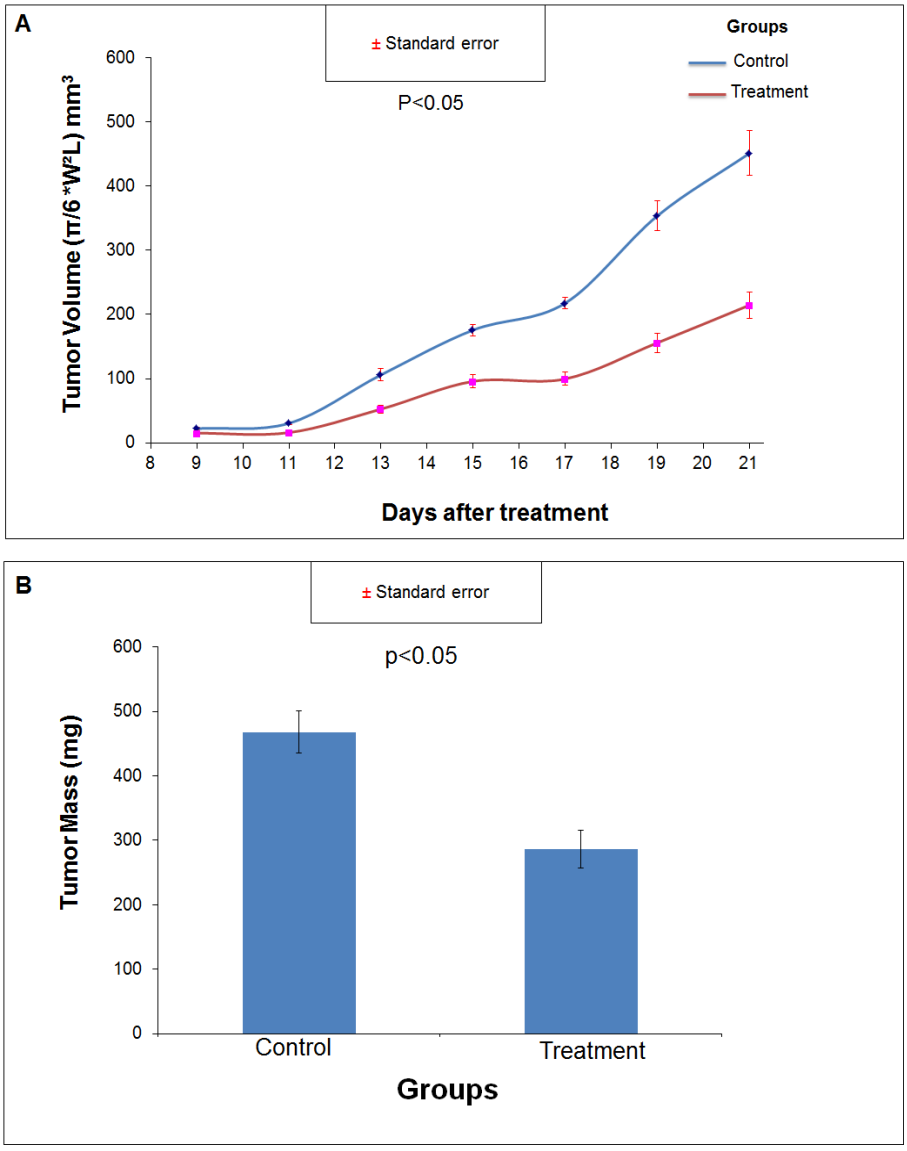

Figure 3-6 Effect on tumor growth from final experiment

A. Calculated tumor volume comparison between different groups from day 9 to day 19. Tumor growth in treatment and luminol groups was delayed over time. Data were analyzed using repeated measures two way ANOVA **B.** Tumor mass comparison between different groups on day 19; luminol showed a significant effect. Data were analyzed using two way ANOVA.

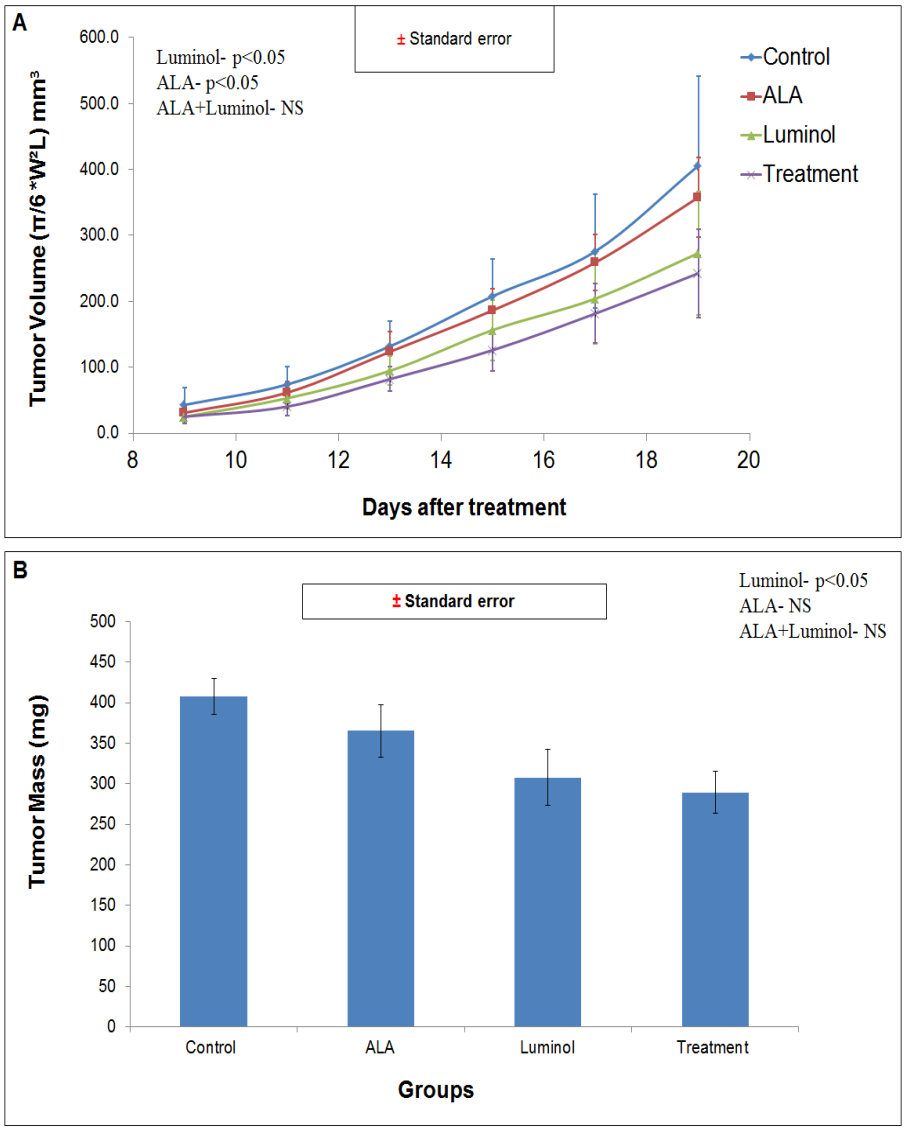

Figure 3-7 Apoptosis Assay

A. Control group. **B.** ALA group. **C**. Luminol group. **D.** Treatment group. **C&D.** Showed more positive apoptotic cells shown in the brown color compared with other groups (qualitative observation). All scale bars 50μm; objective is 10x.

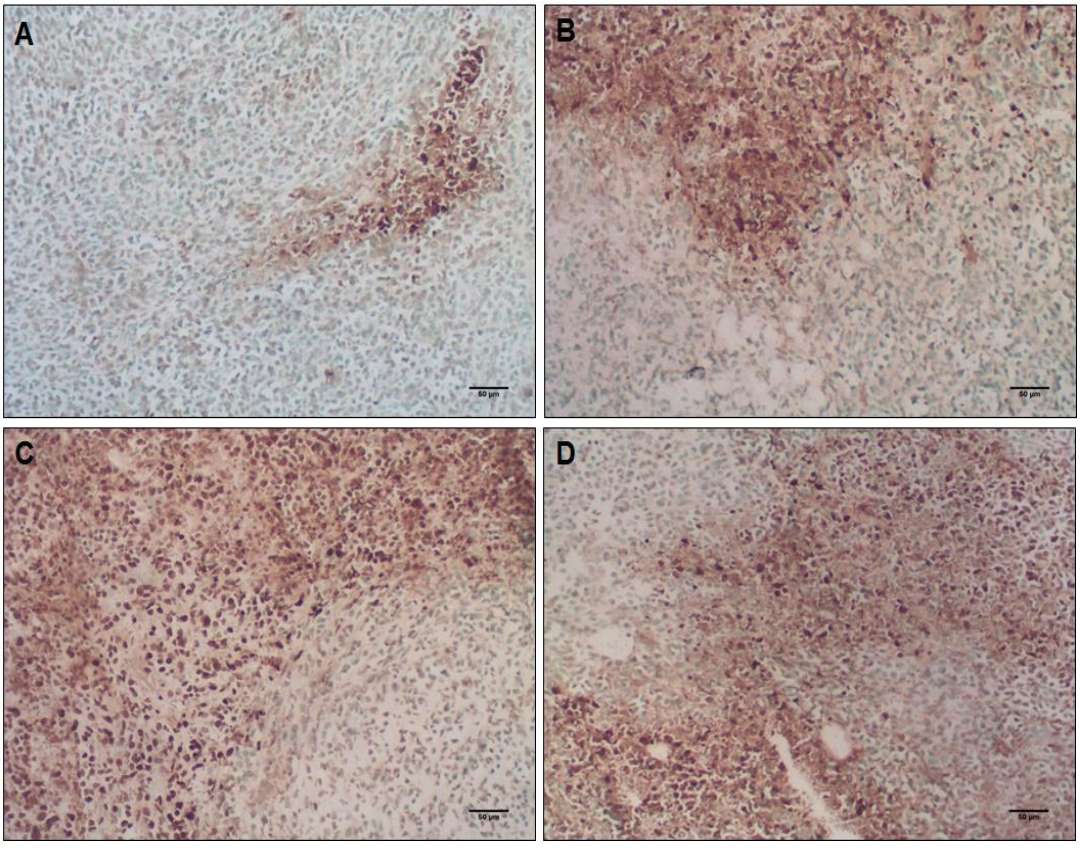

Figure 3-8 Immunohistochemistry of Natural Killer cells

A. Control group. **B.** ALA group. **C**. Luminol group. **D.** Treatment group. All groups showed positive NK cells, shown in red fluorescence; Hoechst counterstain shown in blue fluorescence. **C&D.** Showed more NK cells compared with other groups (qualitative observation). Insets are showing red fluorescence only. All scale bars 50µm; objective is 40x.

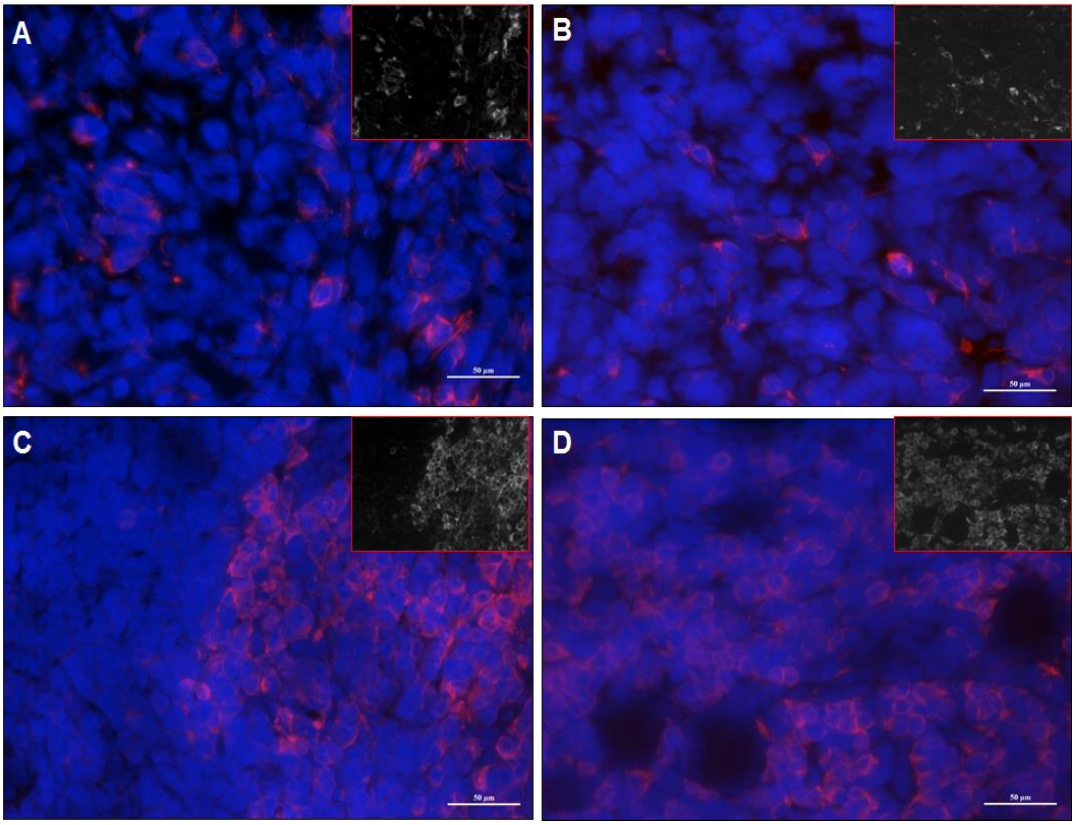

References

1. *American Cancer Society: Global health*. 2008 [cited; Available from: http://www.cancer.org/aboutus/globalhealth/

2. *American Cancer Society: What is cancer?* 2012 [cited 03/21/2012]; Available from: http://www.cancer.org/cancer/cancerbasics/what-is-cancer

3. Hanahan, D. and R.A. Weinberg, *Hallmarks of cancer: the next generation.* Cell, 2011. **144**(5): p. 646-74.

4. *National cancer institute: Understanding Cancer* 2009 [cited 09/30/2009]; Available from: http://www.cancer.gov/cancertopics/understandingcancer/cancer

5. *American Cancer Society: What are the key statistics about breast cancer?* . 2014 [cited 01/31/2014]; Available from: http://www.cancer.org/cancer/breastcancer/detailedguide/breast-cancer-key-statistics.

6. *National cancer institute: Stages of Breast Cancer* 2013 [cited 10/18/2013]; Available from: http://www.cancer.gov/cancertopics/pdq/treatment/breast/Patient/page2.

7. Richie, R.C. and J.O. Swanson, *Breast cancer: a review of the literature.* J Insur Med, 2003. **35**(2): p. 85-101.

8. Egeblad, M., E.S. Nakasone, and Z. Werb, *Tumors as organs: complex tissues that interface with the entire organism.* Dev Cell, 2010. **18**(6): p. 884-901.

9. Hanahan, D. and L.M. Coussens, *Accessories to the crime: functions of cells recruited to the tumor microenvironment.* Cancer Cell, 2012. **21**(3): p. 309-22.

10. Alshetaiwi, H.S., et al., *Luminol-based bioluminescence imaging of mouse mammary tumors.* J Photochem Photobiol B, 2013. **127**: p. 223-8.

11. DeVita, V.T., Jr. and S.A. Rosenberg, *Two hundred years of cancer research.* N Engl J Med, 2012. **366**(23): p. 2207-14.

12. *American Cancer Society: How chemotherapy works.* . 2013 [cited 02/07/2013]; Available from: http://www.cancer.org/treatment/treatmentsandsideeffects/treatmenttypes/chemotherapy/chemotherapyprinciplesanin-depthdiscussionofthetechniquesanditsroleintreatment/chemotherapy-principles-how-chemo-works.

13. *American Cancer Society: How does radiation therapy work?* . 2013 [cited 01/24/2013]; Available from: http://www.cancer.org/treatment/treatmentsandsideeffects/treatmenttypes/radiation/understandingradiationtherapyaguideforpatientsandfamilies/understanding-radiation-therapy-how-does-radiation-therapy-work.

14. BASEL, M.T., *Targeting Cancer Therapy: Using protease cleavage sequences to develop more selective and effective cancer treatments* in *Department of Chemistry* 2010, Kansas State University Manhattan, KS. p. 167.

15. Castano, A.P., P. Mroz, and M.R. Hamblin, *Photodynamic therapy and anti-tumour immunity.* Nat Rev Cancer, 2006. **6**(7): p. 535-45.

16. Glunde, K., A.P. Pathak, and Z.M. Bhujwalla, *Molecular-functional imaging of cancer: to image and imagine.* Trends Mol Med, 2007. **13**(7): p. 287-97.

17. Dolmans, D.E., D. Fukumura, and R.K. Jain, *Photodynamic therapy for cancer.* Nat Rev Cancer, 2003. **3**(5): p. 380-7.

18. Ackroyd, R., et al., *The history of photodetection and photodynamic therapy.* Photochem Photobiol, 2001. **74**(5): p. 656-69.

19. Dougherty, T.J., et al., *Photoradiation therapy. II. Cure of animal tumors with hematoporphyrin and light.* J Natl Cancer Inst, 1975. **55**(1): p. 115-21.

20. Kelly, J.F., M.E. Snell, and M.C. Berenbaum, *Photodynamic destruction of human bladder carcinoma.* Br J Cancer, 1975. **31**(2): p. 237-44.

21. Kelly, J.F. and M.E. Snell, *Hematoporphyrin derivative: a possible aid in the diagnosis and therapy of carcinoma of the bladder.* J Urol, 1976. **115**(2): p. 150-1.

22. Nyst, H.J., et al., *Is photodynamic therapy a good alternative to surgery and radiotherapy in the treatment of head and neck cancer?* Photodiagnosis Photodyn Ther, 2009. **6**(1): p. 3-11.

23. Henderson, B.W. and T.J. Dougherty, *How does photodynamic therapy work?* Photochem Photobiol, 1992. **55**(1): p. 145-57.

24. Siegel, R., D. Naishadham, and A. Jemal, *Cancer statistics, 2012.* CA Cancer J Clin, 2012. **62**(1): p. 10-29.

25. Weissleder, R. and M.J. Pittet, *Imaging in the era of molecular oncology.* Nature, 2008. **452**(7187): p. 580-9.

26. Close, D.M., et al., *In vivo bioluminescent imaging (BLI): noninvasive visualization and interrogation of biological processes in living animals.* Sensors (Basel), 2012. **11**(1): p. 180-206.

27. Kelkar, S.S. and T.M. Reineke, *Theranostics: combining imaging and therapy.* Bioconjug Chem, 2011. **22**(10): p. 1879-903.

28. Siegel, R., D. Naishadham, and A. Jemal, *Cancer Statistics, 2012.* Cancer Journal for Clinicians, 2013: p. 11–30.

29. Kim, J.B., et al., *Non-invasive detection of a small number of bioluminescent cancer cells in vivo.* PLoS One, 2010. **5**(2): p. e9364.

30. Bossmann, S.H. and D.L. Troyer, *Point-of-care routine rapid screening: the future of cancer diagnosis?* Expert Rev Mol Diagn, 2013. **13**(2): p. 107-9.

31. Wu, Y., et al., *Optical imaging of tumor microenvironment.* Am J Nucl Med Mol Imaging, 2013. **3**(1): p. 1-15.

32. Burton, E.R. and S.K. Libutti, *Targeting TNF-alpha for cancer therapy.* J Biol, 2009. **8**(9): p. 85.

33. Alhasan, M.K., et al., *Comparison of optical and Power Doppler ultrasound imaging for non-invasive evaluation of arsenic trioxide as a vascular disrupting agent in tumors.* PLoS One, 2012. **7**(Copyright (C) 2013 American Chemical Society (ACS). All Rights Reserved.): p. e46106.

34. Contag, C.H., et al., *Visualizing gene expression in living mammals using a bioluminescent reporter.* Photochem. Photobiol., 1997. **66**(Copyright (C) 2013 American Chemical Society (ACS). All Rights Reserved.): p. 523-531.

35. Lee, I., et al., *Detection of hydrogen peroxide in vitro and in vivo using peroxalate chemiluminescent micelles.* Bull. Korean Chem. Soc., 2011. **32**(Copyright (C) 2013 American Chemical Society (ACS). All Rights Reserved.): p. 2187-2192.

36. Paroo, Z., et al., *Validating bioluminescence imaging as a high-throughput, quantitative modality for assessing tumor burden.* Mol Imaging, 2004. **3**(Copyright (C) 2013 U.S. National Library of Medicine.): p. 117-24.

37. Sarraf-Yazdi, S., et al., *Use of bioluminescence imaging to detect enhanced hepatic and systemic tumor growth following partial hepatectomy in mice.* Eur J Surg Oncol, 2008. **34**(Copyright (C) 2013 U.S. National Library of Medicine.): p. 476-81.

38. Weissleder, R., et al., eds. *Molecular Imaging: Principles and Practice.* 2010, BC Decker Inc: Hamilton, Ontario, Canada.

39. O'Neill, K., et al., *Bioluminescent imaging: a critical tool in pre-clinical oncology research.* J Pathol, 2010. **220**(3): p. 317-27.

40. Ti-Chen Chen, et al., *Luminol as the light source for in situ photodynamic therapy.* Process Biochemistry, 2012. **47**(12): p. 1903–1908.

41. Radi, R., et al., *Peroxynitrite-induced luminol chemiluminescence.* Biochem J, 1993. **290 (Pt 1)**: p. 51-7.

42. Lundqvist, H. and C. Dahlgren, *Isoluminol-enhanced chemiluminescence: a sensitive method to study the release of superoxide anion from human neutrophils.* Free Radic Biol Med, 1996. **20**(6): p. 785-92.

43. Gross, S., et al., *Bioluminescence imaging of myeloperoxidase activity in vivo.* Nat Med, 2009. **15**(4): p. 455-61.

44. Kricka, L.J. and X. Ji, *4-Phenylylboronic acid: a new type of enhancer for the horseradish peroxidase catalysed chemiluminescent oxidation of luminol.* J Biolumin Chemilumin, 1995. **10**(1): p. 49-54.

45. Chen, W.T., C.H. Tung, and R. Weissleder, *Imaging reactive oxygen species in arthritis.* Mol Imaging, 2004. **3**(3): p. 159-62.

46. Franck, T., et al., *Activation of equine neutrophils by phorbol myristate acetate or N-formyl-methionyl-leucyl-phenylalanine induces a different response in reactive oxygen species production and release of active myeloperoxidase.* Vet Immunol Immunopathol, 2009. **130**(3-4): p. 243-50.

47. Zhang N, F.K., Prakash A, Ansaldi D., *Enhanced detection of myeloperoxidase activity in deep tissues through luminescent excitation of near-infrared nanoparticles.* Nature Medicine, 2013. **19**: p. 500–505.

48. Klebanoff, S.J., *Myeloperoxidase: friend and foe.* J Leukoc Biol, 2005. **77**(5): p. 598-625.

49. Liochev, S.I. and I. Fridovich, *Superoxide and iron: partners in crime.* IUBMB Life, 1999. **48**(2): p. 157-61.

50. Lim, E., K.D. Modi, and J. Kim, *In vivo Bioluminescent Imaging of Mammary Tumors Using IVIS Spectrum.* J Vis Exp, 2009(26): p. e1210.

51. Qureshi, R. and B.A. Jakschik, *The role of mast cells in thioglycollate-induced inflammation.* J Immunol, 1988. **141**(6): p. 2090-6.

52. Granot, Z., et al., *Tumor entrained neutrophils inhibit seeding in the premetastatic lung.* Cancer Cell, 2011. **20**(3): p. 300-14.

53. Inoue, Y., et al., *Comparison of subcutaneous and intraperitoneal injection of d-luciferin for in vivo bioluminescence imaging.* Eur. J. Nucl. Med. Mol. Imaging, 2009. **36**(Copyright (C) 2013 American Chemical Society (ACS). All Rights Reserved.): p. 771-779.

54. Kricka, L.J., *Clinical applications of chemiluminescence.* Analytica Chimica Acta, 2003. **500**(1-2): p. 279-286.

55. Shrestha, T.B., et al., *Stem cell-based photodynamic therapy.* Photochem Photobiol Sci, 2012. **11**(7): p. 1251-8.

56. Maeztu, R., G. Tardajos, and G. Gonzalez-Gaitano, *Natural cyclodextrins as efficient boosters of the chemiluminescence of luminol and isoluminol: exploration of potential applications.* J Phys Chem B, 2010. **114**(8): p. 2798-806.

57. Ahmed, S., et al., *An ultrasensitive and highly selective determination method for quinones by high-performance liquid chromatography with photochemically initiated luminol chemiluminescence.* J Chromatogr A, 2009. **1216**(18): p. 3977-84.

58. Yamaguchi, S., et al., *Evaluation of chemiluminescence reagents for selective detection of reactive oxygen species.* Anal Chim Acta, 2010. **665**(1): p. 74-8.

59. Mahmoudi, M., et al., *Effect of nanoparticles on the cell life cycle.* Chem Rev, 2011. **111**(5): p. 3407-32.

60. DuPre, S.A. and K.W. Hunter, Jr., *Murine mammary carcinoma 4T1 induces a leukemoid reaction with splenomegaly: association with tumor-derived growth factors.* Exp Mol Pathol, 2007. **82**(1): p. 12-24.

61. Mantovani, A., et al., *Cancer-related inflammation.* Nature, 2008. **454**(7203): p. 436-44.

62. Bonecchi, R., M. Locati, and A. Mantovani, *Chemokines and cancer: a fatal attraction.* Cancer Cell, 2011. **19**(4): p. 434-5.

63. Di Carlo, E., et al., *The intriguing role of polymorphonuclear neutrophils in antitumor reactions.* Blood, 2001. **97**(2): p. 339-45.

64. Atai, N.A., et al., *Osteopontin is up-regulated and associated with neutrophil and macrophage infiltration in glioblastoma.* Immunology, 2011. **132**(1): p. 39-48.

65. Khayyata, S., O. Basturk, and N.V. Adsay, *Invasive micropapillary carcinomas of the ampullo-pancreatobiliary region and their association with tumor-infiltrating neutrophils.* Mod Pathol, 2005. **18**(11): p. 1504-11.

66. Shimizu, M., et al., *Roles of CXC chemokines and macrophages in the recruitment of inflammatory cells and tumor rejection induced by Fas/Apo-1 (CD95) ligand-expressing tumor.* Int J Cancer, 2005. **114**(6): p. 926-35.

67. Bekes, E.M., et al., *Tumor-recruited neutrophils and neutrophil TIMP-free MMP-9 regulate coordinately the levels of tumor angiogenesis and efficiency of malignant cell intravasation.* Am J Pathol, 2011. **179**(3): p. 1455-70.

68. Caruso, R.A., et al., *Prognostic value of intratumoral neutrophils in advanced gastric carcinoma in a high-risk area in northern Italy.* Mod Pathol, 2002. **15**(8): p. 831-7.

69. Irie, S., *The treatment of alopecia areata with 3-aminophthal-hydrazide.* Curr Ther Res Clin Exp, 1960. **2**: p. 107-10.

70. Finsen, N.R., *REMARKS on the RED-LIGHT TREATMENT of SMALL-POX: Is the Treatment of Small-pox Patients in Broad Daylight Warrantable?* Br Med J, 1903. **1**(2214): p. 1297-8.

71. Ahn, T.G., et al., *Photodynamic therapy for breast cancer in a BALB/c mouse model.* J Gynecol Oncol, 2012. **23**(2): p. 115-9.

72. Castano, A.P., T.N. Demidova, and M.R. Hamblin, *Mechanisms in photodynamic therapy: part one—photosensitizers, photochemistry and cellular localization.* Photodiagnosis and Photodynamic Therapy, 2004. **1**(4): p. 279–293.

73. Seitz, H.K. and F. Stickel, *Molecular mechanisms of alcohol-mediated carcinogenesis.* Nat Rev Cancer, 2007. **7**(8): p. 599-612.

74. Nowis, D., et al., *Direct tumor damage mechanisms of photodynamic therapy.* Acta Biochim Pol., 2005. **52**: p. 339-52.

75. Dolmans, D.E., et al., *Vascular accumulation of a novel photosensitizer, MV6401, causes selective thrombosis in tumor vessels after photodynamic therapy.* Cancer Res, 2002. **62**(7): p. 2151-6.

76. Wang, H., et al., *Therapeutic and immune effects of 5-aminolevulinic acid photodynamic therapy on UVB-induced squamous cell carcinomas in hairless mice.* Exp Dermatol, 2013. **22**(5): p. 362-3.

77. Balivada, S., et al., *A/C magnetic hyperthermia of melanoma mediated by iron(0)/iron oxide core/shell magnetic nanoparticles: a mouse study.* BMC Cancer, 2009. **10**: p. 119.

78. Wachowska, M., et al., *Aminolevulinic Acid (ALA) as a Prodrug in Photodynamic Therapy of Cancer.* molecules, 2011. **16**(5): p. 4140-4164.

79. Miyake, M., et al., *siRNA-mediated knockdown of the heme synthesis and degradation pathways: modulation of treatment effect of 5-aminolevulinic acid-based photodynamic therapy in urothelial cancer cell lines.* Photochem Photobiol, 2009. **85**(4): p. 1020-7.

80. Amo, T., et al., *Mechanism of cell death by 5-aminolevulinic acid-based photodynamic action and its enhancement by ferrochelatase inhibitors in human histiocytic lymphoma cell line U937.* Cell Biochem Funct, 2009. **27**(8): p. 503-15.

81. Ishizuka, M., et al., *Novel development of 5-aminolevurinic acid (ALA) in cancer diagnoses and therapy.* Int Immunopharmacol, 2010. **11**(3): p. 358-65.

82. Peng, Q., et al., *5-Aminolevulinic acid-based photodynamic therapy: principles and experimental research.* Photochem Photobiol, 1997. **65**(2): p. 235-51.

83. Regula, J., et al., *Photodynamic therapy using 5-aminolaevulinic acid for experimental pancreatic cancer--prolonged animal survival.* 1994. **70**(2): p. 248–254.

84. Bedwell, J., et al., *Fluorescence distribution and photodynamic effect of ALA-induced PP IX in the DMH rat colonic tumour model.* Br J Cancer, 1992. **65**(6): p. 818-24.

85. Peng, Q., et al., *Distribution and photosensitizing efficiency of porphyrins induced by application of exogenous 5-aminolevulinic acid in mice bearing mammary carcinoma.* Int J Cancer, 1992. **52**(3): p. 433-43.

86. Perotti, C., et al., *ALA and ALA hexyl ester induction of porphyrins after their systemic administration to tumour bearing mice.* British Journal of Cancer, 2002. **87**(7): p. 790 – 795.

87. Barbara, W., et al., *HOW DOES PHOTODYNAMIC THERAPY WORK?* . Photochemistry and Photobiology, 1992. **55**(1): p. 145-157.

88. *DeadEnd™ Colorimetric TUNEL System- Promega*. 2009 [cited 03/2009]; Part# TB235:[Available from: http://www.promega.com/~/media/Files/Resources/Protocols/Technical%20Bulletins/0/DeadEnd%20Colorimetric%20TUNEL%20System%20Protocol.pdf.

89. Larina, T.V., et al., *[The immune status and its correction in patients after reconstructive surgeries for cicatricial stenosis of trachea]*. Anesteziol Reanimatol, 2004(5): p. 83-5.

90. Maev, I.V., et al., *[Microcirculatory disorders in chronic erosions of the stomach]*. Klin Med (Mosk), 2003. **81**(6): p. 37-42.

91. *CAM-Cancer-Complementary and Alternative Medicine for cancer: What is Galavit?* 2008 [cited October 1, 2008]; Available from: http://ws.cam-cancer.org/CAM-Summaries/Dietary/Galavit/What-is-it.

92. Zhang, Y. and J.F. Lovell, *Porphyrins as theranostic agents from prehistoric to modern times.* Theranostics, 2012. **2**(9): p. 905-15.

93. Laptev, R., et al., *Intracellular chemiluminescence activates targeted photodynamic destruction of leukaemic cells.* Br J Cancer, 2006. **95**(2): p. 189-96.

94. Anand, S., et al., *Low-dose methotrexate enhances aminolevulinate-based photodynamic therapy in skin carcinoma cells in vitro and in vivo.* Clin Cancer Res, 2009. **15**(10): p. 3333-43.

95. Ortel, B., et al., *Differentiation enhances aminolevulinic acid-dependent photodynamic treatment of LNCaP prostate cancer cells.* Br J Cancer, 2002. **87**(11): p. 1321-7.

96. Anand, S., et al., *Vitamin D3 enhances the apoptotic response of epithelial tumors to aminolevulinate-based photodynamic therapy.* Cancer Res, 2011. **71**(18): p. 6040-50.

97. Hayata, Y., et al., *Hematoporphyrin derivative and laser photoradiation in the treatment of lung cancer.* Chest, 1982. **81**(3): p. 269-77.

98. McCaughan, J.S., Jr., et al., *Palliation of esophageal malignancy with photoradiation therapy.* Cancer, 1984. **54**(12): p. 2905-10.

99. Hayata, Y., et al., *Photodynamic therapy with hematoporphyrin derivative in cancer of the upper gastrointestinal tract.* Semin Surg Oncol, 1985. **1**(1): p. 1-11.

100. Rosenthal, M.A., et al., *Phase I and pharmacokinetic study of photodynamic therapy for high-grade gliomas using a novel boronated porphyrin.* J Clin Oncol, 2001. **19**(2): p. 519-24.

101. Biel, M.A., *Photodynamic therapy and the treatment of head and neck neoplasia.* Laryngoscope, 1998. **108**(9): p. 1259-68.

102. Barr, H., et al., *Photodynamic therapy for colorectal cancer: a quantitative pilot study.* Br J Surg, 1990. **77**(1): p. 93-6.

103. Dimofte, A., et al., *In vivo light dosimetry for motexafin lutetium-mediated PDT of recurrent breast cancer.* Lasers Surg Med, 2002. **31**(5): p. 305-12.

104. Bown, S.G., et al., *Photodynamic therapy for cancer of the pancreas.* Gut, 2002. **50**(4): p. 549-57.

105. Huang, L., T.C. Chen, and F.H. Lin, *Luminol as in situ light source in meso-tetraphenylporphyrin-mediated photodynamic therapy.* Curr Med Chem, 2013. **20**(9): p. 1195-202.

106. Hsu, C.Y., et al., *Bioluminescence resonance energy transfer using luciferase-immobilized quantum dots for self-illuminated photodynamic therapy.* Biomaterials, 2012. **34**(4): p. 1204-12.

Appendix A - Comparison of porphyrin in tumor tissue vs non-tumor tissue

Figure A. To identify endogenous photosensitizer porphyrin that normally accumulates in tumor cells, tumor and non-tumor tissues were collected from mice. Samples were examined by a wide-field fluorescence microscope. Comparison between different groups was analyzed using t-test (not significant).

** This is study has been done at Chemistry department, Kansas State University. Recognitions go to Dr. Thilani Samarakoon, Dipak Giri, Dr. Daniel Higgins, and Dr. Stefan Bossmann.*

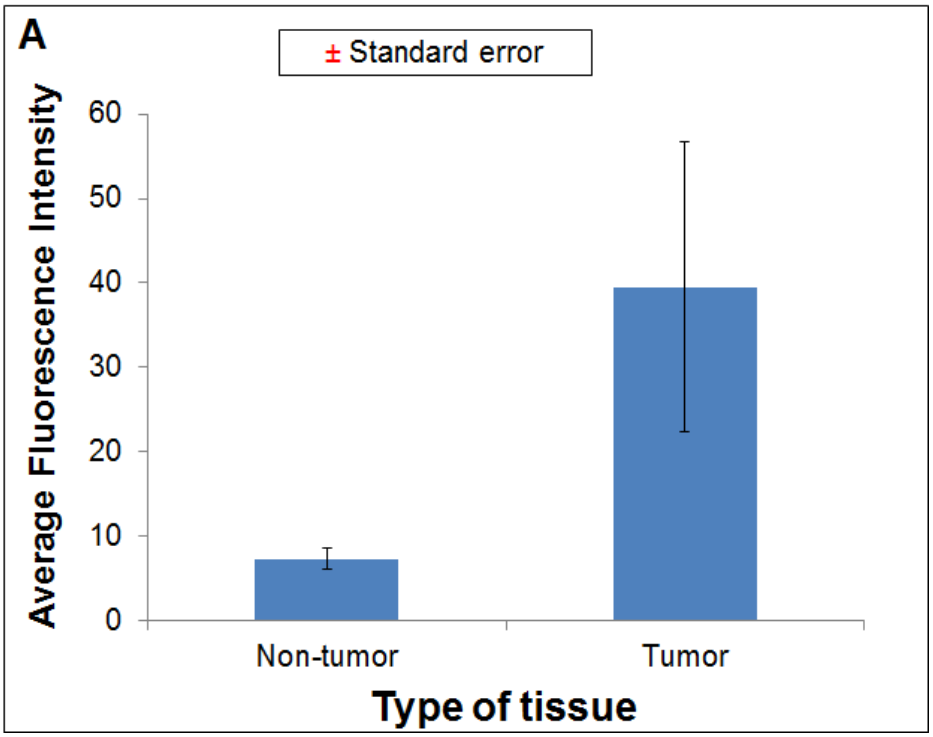

Appendix B - Cytotoxicity of luminol on 4T1 luc2 breast adenocarcinoma cells

Figure B. 4T1 luc2 cells were plated *in vitro* at 12,500 cells/cm^2 and incubated with media containing luminol at concentrations 12.5, 25, 50, 100, 200, 400, or 800 µg/ml. Cell viability was analyzed by using MTT assay after 24 and 48 hrs of incubation. No cytotoxic effects were seen.